GEOLOGICA CARPATHICA, AUGUST 2010, 61, 4, 273–292 doi: 10.2478/v10096-010-0016-1

Geochemistry, petrology and tectonomagmatic significance of basaltic rocks from the ophiolite mélange at the NW External-Internal Dinarides junction (Croatia)

DAMIR SLOVENEC[1], BOŠKO LUGOVIĆ[2] and IRENA VLAHOVIĆ[3]

[1]Croatian Geological Survey, Sachsova 2, HR-10000 Zagreb, Croatia; damir.slovenec@hgi-cgs.hr
[2]Institute of Mineralogy, Petrology and Mineral Deposits, Faculty of Mining, Geology, and Petroleum Engineering, University of Zagreb, Pierottijeva 6, HR-10000 Zagreb, Croatia; blugovic@rgn.hr
[3]GEO-EKO d.o.o., Nikole Pavića 11, HR-10090 Zagreb, Croatia; irena.kloc@geo-eko.hr

(Manuscript received October 28, 2009; accepted in revised form March 11, 2010)

Abstract: At the NW inflexion of the Sava-Vardar Suture Zone ophiolite mélanges, known as the Kalnik Unit, form the surface of the slopes of several Pannonian inselbergs in the SW Zagorje-Mid-Transdanubian Zone. The Mt Samoborska Gora ophiolite mélange, thought to be a part of the Kalnik Unit, forms a separate sector obducted directly onto Dinaric Triassic carbonate sediments. Basaltic rocks, the only magmatic rocks incorporated in the mélange, include Middle–Triassic (Illyrian–Fassanian) alkali within-plate basalts and Middle Jurassic (uppermost Bathonian–Lower Callovian) tholeiitic basalts. The latter sporadically constitute composite olistoliths, and are geochemically divided into N-MORB-like (high-Ti basalts) and transitional MORB/IAT (medium-Ti basalts). These geochemically different rocks suggest crystallization at various tectonomagmatic settings, which is also indicated by the rock paragenesis and host clinopyroxene compositions. Alkali basalts reflect melts derived from an OIB-type enriched mantle source [Ti/V = 62.2–82.4; $(La/Lu)_{cn}$ = 6.4–12.8] with Nd-Sr isotope signatures close resembling the Bulk Earth [$\varepsilon_{Nd(T=235\ Ma)}$ = + 1.6 to + 2.5]. They are recognized as pre-ophiolite continental rift basin volcanic rocks that closely predate the opening of the Repno oceanic domain (ROD) of the Meliata-Maliac ocean system. The high-Ti and medium-Ti basalts from composite blocks derived from a similar depleted mantle source ($\varepsilon_{Nd(T=165\ Ma)}$ = + 6.01 vs. + 6.35) succesively metasomatized by expulsion of fluids from a subducting slab leading to a more pronounced subduction signature in the latter [Ti/V = 31.6–44.8 and $(Nb/La)_n$ = 0.67–0.90 vs. Ti/V = 21.5–33.9 and $(Nb/La)_n$ = 0.32–0.49]. These composite blocks indicate crust formation in an extensional basin spreading over the still active subducting ridge. The majority of high-Ti basalts may represent the fragments of older crust formed at a spreading ridge and incorporated in the mélange of the accretionary wedge formed in the proto-arc–fore-arc region. The Mt Samoborska Gora ophiolite mélange represents the trailing edge of the Kalnik Unit as a discrete sector that records the shortest stage of tectonomagmatic evolution related to intraoceanic subduction in the ROD.

Key words: Triassic–Jurassic, Croatia, Samoborska Gora Mts, proto-arc extension, back-arc spreading, alkali within-plate basalts, tholeiitic basalts, ophiolite mélange.

Introduction

Mélanges are by consensus understood as chaotic tectono-sedimentary complexes that have been initially deposited by tectonically induced sedimentary processes in an accretionary wedge from a fore-arc region. Consequently, an ophiolite mélange mostly incorporates mixed magmatic material derived from both interfaced oceanic sides. Because of a long tectonic history of obduction various lithoclasts representing diferent tectonomagmatic stages of an oceanic basin may be identified in the final product. Many mélanges are overlain by slices of coherent fragments of genetically related oceanic lithosphere (ophiolites) which may include lithologies not found in the associated mélange and vice versa. The comparative petrological and geochemical investigations of magmatic inclusions found in a mélange combined with analogue rocks of related ophiolite sequences always provide important, although incomplete constraints on the tectonomagmatic evolution of an oceanic basin and its segments from continental rifting to opening and formation of oceanic lithosphere through spreading and convergence till the final ophiolite emplacement.

In the SW segment of the Zagorje-Mid-Transdanubian Zone (ZMTDZ) of the Sava Suture Zone the tectono-sedimentary ophiolite mélanges lacking overthrusted ophiolites are commonly found as individual sectors on the surface of slopes of intra-Pannonian inselbergs of Kalnik, Ivanščica and Medvednica (Pamić & Tomljenović 1998, and references therein). On account of similar textural features all these mélange sectors are assumed to constitute a single unit (Babić et al. 2002) referred to as the Kalnik Unit (Hass et al. 2000), which brings strong evidence for a discrete oceanic domain (Repno oceanic domain = ROD) within the Meliata-Maliac ocean system (Babić et al. 2002; Goričan et al. 2005; Slovenec & Lugović 2008, 2009). However, excluding the Mt Medvednica ophiolite mélange where magmatic megaclasts or olistoliths have been geochemically studied in detail and stages of terminal spreading and initial convergence were dated by isotopes (Lugović et al. 2007; Slovenec & Lugović 2008, 2009) other sectors still wait for such complementary data that would confirm other sectors as true integral parts of the Kalnik Unit.

The Samoborska Gora ophiolite mélange has a peculiar position as it was obducted directly onto Triassic sediments of

the Adria amagmatic passive continental margin and traces the headmost edge of a larger mélange unit. This mélange is separated from the Medvednica ophiolite mélange by the regional Sava fault and thus it is not clear whether it constitutes a discrete ophiolite mélange unit, or represents a detached segment of the Kalnik Unit. Present study revealed that besides apparently similar blocks of magmatic rocks as in the other mélange sectors of ZMTDZ, Mt Samoborska Gora mélange includes blocks of within-plate alkali basalts which were not up to now identified in other mélange sectors. However, during the testing of correlation between ophiolitic blocks from the Mt Samoborska Gora and those from the Mt Medvednica, similar alkali basalts were also found for the first time in the ophiolite mélange of the Mt Medvednica. In this work we performed geochemical and petrological characterization of almost all ophiolitic blocks from the Mt Samoborska Gora with the purpose of testing possible correlation with Mt Medvednica ophiolite rock fragments. The age of massive lava blocks was obtained by isotope age determination, and the age of pillow lavas was determined from the fauna content in the intrapillow matrix or from atop pillow lavas associated cherts. New data were utilized to infer or improve the geodynamic evolution of the oceanic segment(s) from which ophiolites of Mts Samoborska Gora and Medvednica have been derived.

Geological outlines

Samoborska Gora is the cornerstone that links the External Dinarides, Southern Alpine units, southwestern tip of the Zagorje-Mid-Transdanubian Zone (ZMTDZ) as a part of the Sava-Vardar Suture Zone (SVSZ) and the continental block of the Tisia Unit (Fig. 1A). Its exact tectonic position in the framework of Alpine-Dinaric-Pannonian triple junction zone sensu Hass & Kovács (2001) is not clearly explained yet (e.g. Pamić & Tomljenović 1998; Tari & Pamić 1998; Hass et al. 2000; Pamić 2002; Babić et al. 2002; Goričan et al. 2005; Schmid et al. 2008; Robertson et al. 2009). However, a position within the transitional zone between the External and Internal Dinarides seems to be most acceptable (Placer 1999).

Mt Samoborska Gora consists of two tectonostratigraphic units, the pre-Eocene Žumberak Autochthony overthrusted by the south-west vergent Žumberak Nappe (Šikić et al. 1979) (Fig. 1B). The Žumberak Autochthony shows a sedimentary succession identical to the eastern border of Adriatic carbonate platform (Tomljenović 2002). The oldest rocks of the Žumberak Autochthony are Permian molasse-type clastic rocks which are unconformably overlain by Lower Triassic clastic rocks followed by Upper Triassic carbonate rocks with minor cherts (Herak 1956; Šikić et al. 1979). Locally, the Late Anisian sedimentary succession may be interstratified with acidic pyroclastic rocks (Goričan et al. 2005). The ophiolite mélange is thrusted onto Middle Triassic carbonates. The age of the ophiolite mélange is supposed to be Middle Jurassic to Hauterivian by analogy with similar mélanges from the Kalnik Unit (Babić et al. 2002). Unlike in the Mt Medvednica, where the Paleozoic-Triassic sedimentary succession was subjected to an Early Cretaceous low grade metamorphic overprint (Belak et al. 1995, with references) related to obduction of an intraoceanic island arc (Lugović et al. 2006), the Mt Samoborska Gora analogue succession lacks any metamorphism. The youngest rocks of the Žumberak Autochthony are the Late Campanian–Paleocene alluvial and delta fan deposits (Šikić et al. 1979; Fig. 1C) which in many lines of evidence resemble post-ophiolitic Gossau- or Ugar-type sedimentary sequence.

The Žumberak Autochthony is thrusted by the Žumberak Nappe composed of a thick sedimentary succession showing identical lithostratigraphic sequences as in the Žumberak Autochthony (Fig. 1B). Top-WSW thrusting, internal imbrication and folding of the Žumberak Autochthony related to an Eocene deformational event affected Mt Samoborska Gora and Mt Medvednica (D3 event of Tomljenović 2002). The Žumberak Nappe consists of three individual thrust sheets (Japetić, Cirnik and Vrhovčak) which represent the uppermost pre-Neogene structural units (Šikić et al. 1979). The best exposure of the ophiolite mélange is under the Vrhovčak thrust sheet where fragments of basaltic rocks were sampled in detail. The Neogene and Quaternary strata mostly unconformably overlay the pre-Eocene basement on the southeastern slopes; on the northern slopes the basement rocks are transgressively overlain by the younger strata (Fig. 1C).

The ophiolite mélange of the Mt Samoborska Gora shows characteristics of a chaotic olistostrome complex mixed with fault-bounded fragments of different lithologies varying in size from a few centimeters to several tens of meters set in a strongly sheared pelitic-siltous continent derived matrix. Ophiolite mélange contains clasts of greywacke, minor shale, reddish and greyish cherts, scarce limestones along with fragments of ophiolitic basaltic rocks (Herak 1956; Brajdić & Bukovec 1989; Kloc 2005). Other ophiolite rocks are notably absent. Massive lavas predominate over pillow lavas. The fragments are homogeneous in the term of texture and geochemistry with the exception of a unique, texturally uniform hektometer sized block (Fig. 1C, location 2) composed of tholeiitic high-Ti and medium-Ti basaltic rocks. K-Ar measurement on plagioclase separate from the high-Ti segment of this composite block has yielded an uppermost Bathonian–Early Callovian age of 165.4 ± 5.8 Ma (Balogh 2009; unpublished). The observed age of sedimentary rock fragments range from Middle Triassic for "exotic" limestones to Middle Jurassic for greyish radiolarian cherts (Goričan 2008, unpublished).

Fragments of alkali basalts are concentrated in the easternmost part of the Mt Samoborska Gora ophiolite mélange (Fig. 1C; locations 10–13) where reddish radiolarian cherts crop out above massive alkali basalts (Fig. 1; location 12). The radiolarian assemblage of these cherts indicates Middle Triassic age (Goričan 2008, unpublished). Assuming that they are integrated in a coherent block, they would represent the oldest fragments incorporated in the ophiolite mélange of Mt Samoborska Gora.

In the westernmost part of the Mt Medvednica ophiolite mélange near the village Gornja Bistra (Fig. 1B) crop out the hectometer large block of similar massive alkali basalts and their pillow lavas with interpillow pelagic limestones of Illyrian-Fassanian age of Middle Triassic (Halamić et al. 1998). For

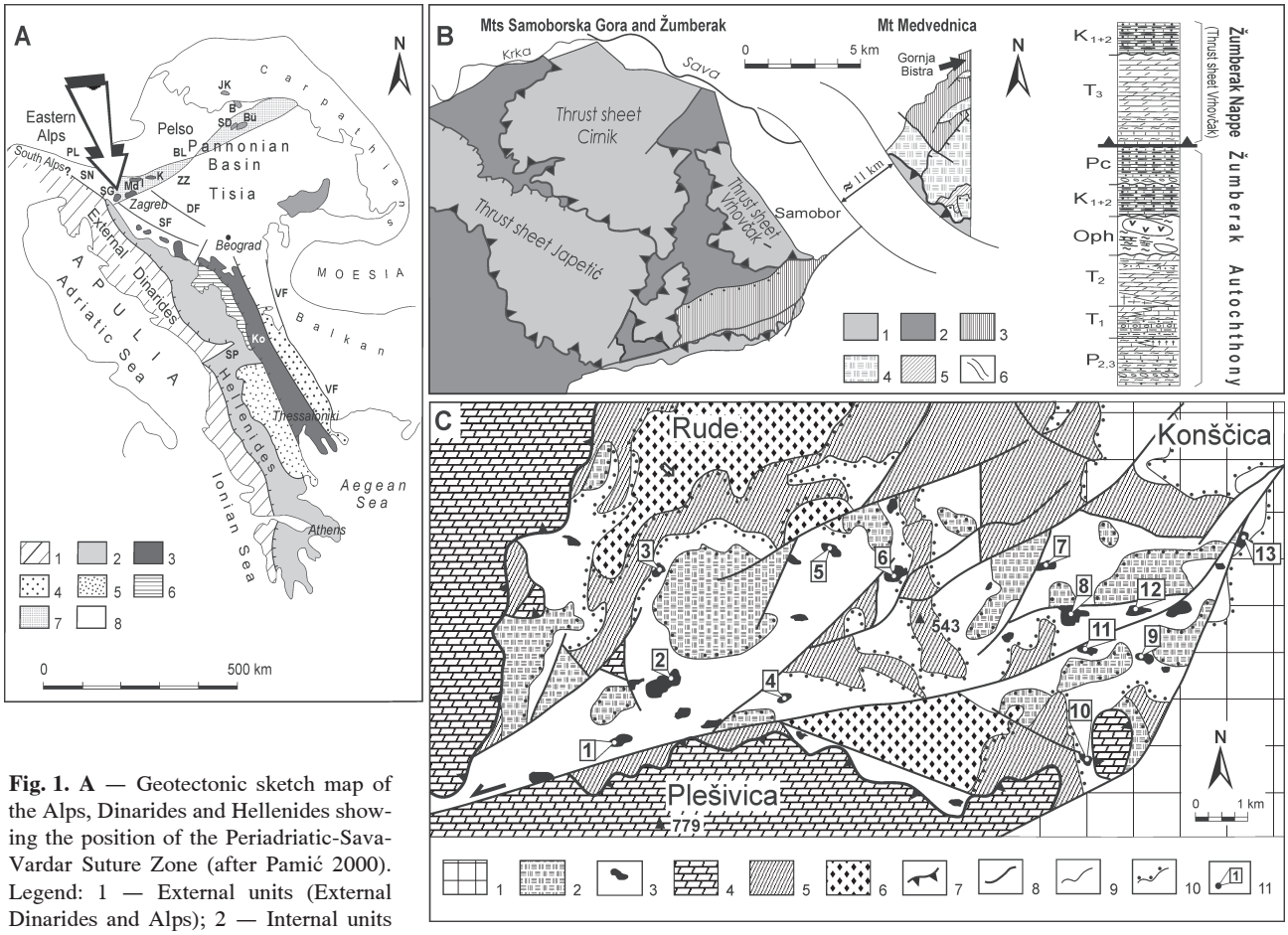

Fig. 1. A — Geotectonic sketch map of the Alps, Dinarides and Hellenides showing the position of the Periadriatic-Sava-Vardar Suture Zone (after Pamić 2000). Legend: 1 — External units (External Dinarides and Alps); 2 — Internal units [Passive continental margin, Central Dinaride Ophiolite Belt (CDOB), Mirdita Zone]; 3 — Periadriatic-Sava-Vardar Zone; 4 — Serbo-Macedonian Massif; 5 — Pelagonides; 6 — Golija Zone; 7 — Zagorje-Mid-Transdanubian Zone; 8 — Pannonian Basin. Faults: BL — Balaton; DF — Drava; PL — Periadriatic; SF — Sava; SP — Scutari-Peć; SN — Sava Nappe; ZZ — Zagreb-Zemplín. Mountains: I — Ivanščica; K — Kalnik; Ko — Kopaonik; Md — Medvednica; SG — Samoborska Gora; SD — Szarvaskő-Darnó; Bü — Bükk; B — Bódva Valley; JK — Jaklovce. **B** — Interpretations of overthrust relations in the Mt Samoborska Gora and western part of the Mt Medvednica (after Šikić & Basch 1975 and Šikić et al. 1978, 1979; taken from Tomljenović 2002). Legend: 1 — Žumberak Nappe; 2 — Žumberak Autochthony; 3 — Ophiolite mélange (Oph); 4 — Upper Cretaceous-Paleocene sediments; 5 — Lower Cretaceous metamorphic complex; 6 — picture break. **C** — Simplified geological map of the Mt Samoborska Gora (modified after Šikić et al. 1978 and Tomljenović 2002). Legend: 1 — Neogene and Quaternary sedimentary rocks; 2 — Upper Cretaceous-Paleocene flysch; 3 — ophiolite mélange with blocks of basalt (black fields) and Triassic-Jurassic radiolarites, sandstones and shales (not separated on the map); 4 — Upper Triassic dolomites and limestones; 5 — Middle–Lower Triassic dolomites, limestones, cherts and clastic rocks (shale, siltite and sandstone); 6 — Upper Permian clastic rocks (conglomerate, sandstone, siltite and shale), limestones, dolomites and gypsum; 7 — reverse or thrust faults; 8 — normal faults; 9 — geological contact line; 10 — discordance line, tectonic-erosion discordance; 11 — sample location (1 = js-73/1; 2 = jf-33/2, jf-34, t-23b/1, t-23b/2; 3 = sas-8; 4 = js-60; 5 = 92-18; 6 = sat-242; 7 = t-56/1; 8 = sas-202; 9 = sas-206; 10 = 92-20, 92-21, 92-22, 92-23, 92-25, 92-30; 11 = sas-203; 12 = sas-210; 13 = 92-16).

the purpose of correlation the data on these rocks were integrated in the present work.

The Mt Samoborska Gora ophiolite mélange in many respects shares the overall textural characteristics of the Mt Medvednica ophiolite mélange (Babić et al. 2002; Slovenec & Pamić 2002, and references therein) suggesting that both mélanges may have formed by accretion along a discrete sediment-starved trench and were tectonized during the onset of obduction. The pre-Neogene Mt Medvednica basement experienced regional-scale tectonic transport from the NW, and 130° clockwise rotation during the Oligocene–earliest Miocene (Tomljenović et al. 2008), which caused its recent perpendicular orientation to the overall NW-SE Dinaric structural trend (Fig. 1A). Therefore, the ophiolite mélange of Mt Samoborska Gora should be tested as a potential prolongation of the Mt Medvednica ophiolite mélange, and so of the Kalnik Unit.

Like elsewhere in the Dinarides the onset of tectonic reworking of Mt Samoborska Gora ophiolitic mélange took place successively during and after the first ophiolite emplacement onto the Adria continental margin (Schmid et al. 2008; Robertson et al. 2009, and references therein) and continued during the Cretaceous until the Senonian as confirmed by mantle peridotite clasts in the Campanian basal conglomerates (Halamić 1998) and subaerial weathering of peridotites to the Ni-lateritic crust (Palinkaš et al. 2006).

Analytical techniques

Mineral analyses from eleven representative samples were performed at the Mineralogisches Institut, Universität Heidelberg, using a CAMECA SX51 electron microprobe equipped with five wavelength-dispersive spectrometers. The operating parameters were 15 kV accelerating voltage, 20 nA beam current, ~1 μm beam size (10 μm for plagioclase) and 10 s counting time for all elements. Natural minerals, oxides (corundum, spinels, hematite and rutile) and silicates (albite, orthoclase, anorthite and wollastonite) were used for calibration. Raw data for all analyses were corrected for matrix effects with the PAP algorithm (Pouchou & Pichoir 1984, 1985) implemented by CAMECA. Formula calculations were done using a software package authorized by Hans-Peter Meyer (Mineralogisches Institut, Universität Heidelberg). The mineral composition of higly altered samples was analysed by X-Ray diffraction on powdered samples (XRD).

Bulk-rock powders for chemical analyses of twenty five samples were obtained from rock chips free of visible veins. Six samples with amygdulas or calcite veins were dissolved in Na-acetate (NaOAc) at pH around 6 controlled by acetic acid (HAc).

Major elements were measured by ICP and all trace elements by ICP-MS at Activation Laboratories in Ancaster, Canada. A series of international standards were used to construct calibration curves. Referent samples W2 and WMG-1 were run as unknowns. Major element and trace element concentrations were measured with accuracy better than 1 % and 5 %, respectively.

Isotopic analyses were done in CRPG in Vandoeuvre, France on Finnigan MAT 262 mass spectrometer following the procedure described in Hart & Brooks (1977). Sr fractions were deposited on single W filaments and TaF_5–H_3PO_4 was added as an activator. Double filaments (Ta for emission, Re for ionization) were used for Nd analyses. Nd fractions were deposited on the Ta filaments, with H_3PO_4 added as an activator. All analyses were made in multi-dynamic mode, using software developed by Spectromat. An exponential law was used for fractionation correction. Normalizing ratios of $^{86}Sr/^{88}Sr = 0.1194$ and $^{146}Nd/^{144}Nd = 0.7219$ were assumed. The $^{87}Sr/^{86}Sr$ value for the NBS 987 Sr standard for the period of measurement was 0.710254 ± 0.000028 (2σ, n = 92). The $^{143}Nd/^{144}Nd$ value for the La Jolla Nd standard was 0.511841 ± 0.000020 (2σ, n = 22). An in-house Nd standard was also analysed during this period, yielding a $^{143}Nd/^{144}Nd$ ratio of 0.511110 ± 0.000020 (2σ, n = 100), consistent with the value obtained for this standard over the past 15 years. Total procedural blanks were ~700 pg and ~300 pg for Sr and Nd, respectively.

Petrography and mineral chemistry

Extrusive rocks from the Mt Samoborska Gora ophiolite mélange comprise pillow lavas and massive lavas of high-Ti and medium-Ti tholeiitic and alkali basalt composition, respectively. Pillows of amoeboidal shape with tortoise shell joints were noticed occasionally (Fig. 1C, location 2). In spite of polyphase alterations which may be severe, igneous textures are preserved in all samples.

Tholeiitic extrusives are mostly aphyric and composed of plagioclase, clinopyroxene, Fe-Ti oxide, spinel and accessory apatite (Fig. 2A,B). Plagioclase from the high-Ti group shows normal zoning with labradorite core and andesine rim ranging in overall composition from An_{71-54} to $An_{48.6-31.5}$, respectively. The highest individual core to rim variation is An_{71-40} (Table 1). In the medium-Ti tholeiitic group, igneous plagioclase is altered to albite ($An_{0.1-2.9}$) or peristerite ($An_{\sim 7}$) with minor sericite, calcite, prehnite, analcime and pumpellyite, and therefore the rocks may be classified as spilites. Clinopyroxene shows two stages of alteration. Some clinopyroxenes from the high-Ti samples show deuteric alterations to ferohornblende-feroedenite and in both geochemical groups are partly hydrothermally altered to chamosite-clinochlore, epidote and pumpellyite (Fig. 2A,B; Table 1). In the high-Ti basalts Fe-Ti oxide is ulvöspinel-magnetite ($Usp_{16.6-46.8}Mgt_{50.2-79.0}Spl_{0.9-7.5}$) coexisting with ilmenite ($Ilm_{92.8-96.2}Hem_{3.8-7.2}$) whilst in the medium-Ti basalts low-Ti chromian spinel (Mg# = 70–77, Cr# = 26–30, $TiO_2 < 0.38$ wt. %) crystallized along with minor Fe-Ti oxides (Table 1). The *pillow lavas* are aphyric to slightly plagioclase-phyric or plagioclase-clinopyroxene-phyric. The pillows show characteristic increasing crystallinity from the outer chilled margin, showing plumose-variolitic to hypocrystalline porphyric texture, to the hollocrystalline core with aphyric ophitic to intergranular texture. Calcite and/or chlorite filled amygdaloidal tholeiitic pillow lavas are rarely observed. *Massive lavas* are mostly aphyric and show fine- to coarse-grained ophitic to intergranular texture undistinguishable from pillow core. Petrographical evidence in the tholeiitic basalts suggests the following order of crystallization: plagioclase → clinopyroxene + plagioclase + Fe-Ti oxides (Fig. 2A). Additionally, in some medium-Ti pillow and massive basalts spinel coexists with the early fractionated plagioclase whilst rare Fe-Ti oxides are confined in matrix.

Alkali basalts from the Mts Samoborska Gora and Medvednica ophiolite mélanges show similar aphyric quenched textures suggesting a fast cooling rate at the time of effusion. In thin sections they show spinnifex- to variolitic-like domains (variolites) formed by sheaf- or plumose-textured pinkish clinopyroxene intergrown with acicular plagioclase with interstitial glass infillings (Fig. 2C). Primary spinel (Mg# = 59–62, Cr# = 42–46; Table 1) and Ti-magnetite are accessory phases. In all samples plagioclase is completely altered to albite, prehnite and occasionally to pumpellyite. Clinopyroxenes from the Mt Medvednica alkali basalts are fresh whilst those from the Mt Samoborska Gora are always altered to chlorite. Glass is devitrified to palagonitic mesostasis and consists of chlorite, calcite, hematite, prehnite, pumpellyite and titanite. The lavas are amygdaloidal with up to 30 % amygdals filled by calcite suggesting relatively shallow water effusion compared to tholeiitic lavas.

Clinopyroxene chemistry. Selected matrix clinopyroxene compositions from the analysed tholeiitic and alkali rocks are shown in Table 2 and all are plotted in the classification diagram in Fig. 3.

Clinopyroxenes from *tholeiitic host rocks* show normal and reverse zoning. Normally zoned grains have homogeneous

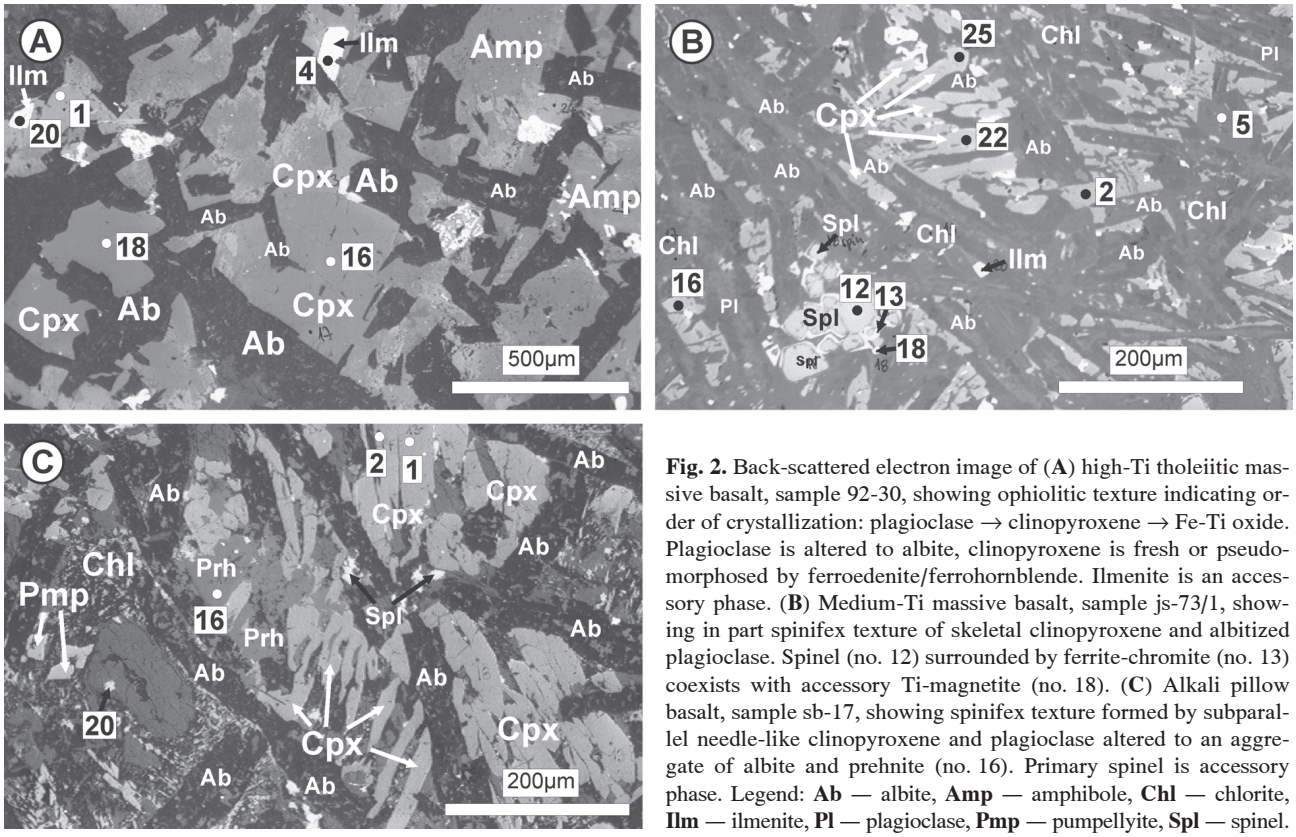

Fig. 2. Back-scattered electron image of (**A**) high-Ti tholeiitic massive basalt, sample 92-30, showing ophiolitic texture indicating order of crystallization: plagioclase → clinopyroxene → Fe-Ti oxide. Plagioclase is altered to albite, clinopyroxene is fresh or pseudomorphosed by ferroedenite/ferrohornblende. Ilmenite is an accessory phase. (**B**) Medium-Ti massive basalt, sample js-73/1, showing in part spinifex texture of skeletal clinopyroxene and albitized plagioclase. Spinel (no. 12) surrounded by ferrite-chromite (no. 13) coexists with accessory Ti-magnetite (no. 18). (**C**) Alkali pillow basalt, sample sb-17, showing spinifex texture formed by subparallel needle-like clinopyroxene and plagioclase altered to an aggregate of albite and prehnite (no. 16). Primary spinel is accessory phase. Legend: **Ab** — albite, **Amp** — amphibole, **Chl** — chlorite, **Ilm** — ilmenite, **Pl** — plagioclase, **Pmp** — pumpellyite, **Spl** — spinel.

cores and show decreasing Al^{VI}/Al^{IV}, Mg# and generally increasing Ti to the grain periphery. In reverse zoned grains the patterns show opposite compositional variations. In Fig. 3 clinopyroxene reveals two compositional groups. The majority of clinopyroxene from high-Ti host rocks stretch in the field of augite ($Wo_{38.1-42.8}En_{40.9-48.9}Fs_{10.6-20.1}$) and forms a compositional trend concordant with analogue rocks from Mt Medvednica ophiolite mélange described by Slovenec & Lugović (2009). On the contrary, the clinopyroxenes hosted in the largest block from the Mt Samoborska Gora ophiolite mélange (Fig. 1C; location 2), composed of high-Ti basalts (sample jf-33/2) associated with medium-Ti basalts (sample jf-23/b2) as well as clinopyroxenes from an individual medium-Ti block (Fig. 1C; location 1 sample js-73/1) form a separate compositional trend with a distinctly higher Wo- and Fs-content. Clinopyroxenes hosted in the high-Ti rock from the block shows transitional diopside-augite composition ($Wo_{43.4-46.3}En_{39.7-413}Fs_{13.4-16.8}$) whilst those from the medium-Ti rock entity stretch along the line separating the hedenbergite-augite compositional fields ($Wo_{43.7-46.1}En_{21.9-26.6}Fs_{28.4-34.3}$). The clinopyroxenes hosted in both analysed medium-Ti rocks compared with clinopyroxene compositions from high-Ti rock entity of the composite blok, contain more TiO_2 (1.58–3.05 wt. % vs. 1.25–1.69 wt. %), Na_2O (0.45–0.59 wt. % vs. 0.35–0.43 wt. %), and generally higher Al_2O_3 (3.49–7.19 wt. % vs. 3.38–5.51 wt. %) (Fig. 3A–C), and show significantly Fe-enriched (Mg#=43.2–74.2.0 vs. 74.6–80.2). This is not expected for clinopyroxene hosted in the rocks derived from a more depleted source.

Clinopyroxenes of *alkali basalts* from Mt Samoborska Gora are completely altered and only the clinopyroxene composition from Mt Medvednica alkali basalts are shown in Table 2. These clinopyroxenes are normally zoned and show diopsidic composition ($Wo_{47.4-49.6}$ $En_{30.1-36.5}Fs_{14.3-22.5}$; Fig. 3). Their high content of other-than-quadrilateral components (TiO_2=2.99–4.17 wt. %; Al_2O_3=5.89–7.40 wt. %; Fig. 4A–B) clearly reflected the alkali non-orogenic nature of the host rocks (Leterrier et al. 1982). High-Ti content of clinopyroxene is favoured by cooling rate of crystallization, magma chemistry and cotectic opaque phase (Tracy & Robinson 1977). High titanium content in the clinopyroxene is consistent with enriched composition of relatively primitive alkali basaltic magma, coexisting low-Ti spinel (TiO_2 >1.6 wt. %) and fast cooling rate as suggested by quenching textures of host pillow basalts.

Bulk-rock chemistry

Chemical compositions of the analysed rocks are shown in Table 3. As virtually shown by petrography and the high LOI of the samples (up to 8.46 wt. %), and by experience from similar rocks elsewhere (e.g. Pearce & Cann 1973; Thomson 1991) significant element mobility is expected to occur in most of the samples. Here, potential element mobility was tested by plotting their concentrations against Zr selected as differentiation index (Fig. 5).

For the tholeiitic rock suite, except for TiO_2 and P_2O_5 which are positively correlated with Zr, the major elements do not

Table 1: Selected microprobe analyses and formulae of feldspars, amphibole, chlorite, spinel, ulvöspinel-magnetite and ilmenite from the tholeiitic and alkali volcanic rocks in the Mts Samoborska Gora and Medvednica ophiolite mélange.

	Feldspar				Amphibole				Chlorite			Magnetite-ulvöspinel			Chromian Spinel				Ilmenite	
Sample	jf-33/2	jf-33/2	js-73/1	sat-210	92-18	92-20	92-22	92-30	92-16	92-22	jf-33/2	92-18	92-21	92-22	js-73/1	t-23b/2	sb-9	sb-17	92-30	92-30
Anal. nr.	12	13	5	2	9	32	9	1	10	8	14	31	8	18	12	7	24	20	4	20
Site	c	r	c	c	c	c	r	c	r	c	c	c	c	c	c	c	c	c	c	c
Rock type	PB	PB	MB	MB	MB	MB	PB	MB	MB	PB	PB	MB	MB	PB	MB	PB	MB	PB	MB	MB
Rock affinity	Th	Th	Th	Alk	Th	Th	Th	Th	Alk	Th	Th	Th	Th	Th	Th	Th	Alk	Alk	Th	Th
SiO_2	50.30	57.93	66.42	69.38	45.17	50.55	48.73	47.40	31.60	27.68	38.80	0.11	0.04	0.98	0.11	0.09	0.04	0.09	0.02	0.02
TiO_2	–	–	–	–	2.05	0.67	0.99	1.17	0.03	0.04	0.02	9.48	10.49	14.85	0.33	0.38	1.61	1.26	49.48	49.49
Al_2O_3	30.61	25.64	21.42	19.57	6.65	2.54	3.97	4.25	17.50	16.06	14.64	1.67	2.94	0.53	41.00	39.50	26.51	28.50	0.00	0.00
Cr_2O_3	–	–	–	–	0.00	0.07	0.02	0.03	0.00	0.00	0.01	0.08	0.07	0.06	24.72	22.73	33.48	32.38	0.06	0.03
Fe_2O_3	0.59	0.97	0.29	0.24	–	–	–	–	–	–	–	48.00	44.54	36.85	3.94	6.87	7.41	7.27	5.66	5.43
FeO	–	–	–	–	22.40	23.38	22.29	23.91	10.38	30.06	10.70	39.10	40.29	44.88	10.76	12.72	15.95	15.24	38.10	43.02
MnO	–	–	–	–	0.31	0.43	0.34	0.33	0.38	0.24	0.21	0.53	0.56	0.33	0.12	0.11	0.14	0.09	5.87	0.82
MgO	–	–	–	–	9.23	11.25	10.18	9.43	24.96	12.16	22.60	0.05	0.09	0.17	18.12	16.63	13.78	14.10	0.07	0.38
CaO	14.42	8.17	1.63	0.03	9.27	7.73	9.03	9.23	0.32	0.22	1.11	0.31	0.06	0.40	0.03	0.08	0.07	0.46	0.28	0.00
Na_2O	3.20	6.64	11.04	11.82	2.34	1.08	1.60	1.68	0.02	0.01	0.05	–	–	–	–	–	–	–	–	–
K_2O	0.05	0.12	0.03	0.01	0.22	0.17	0.17	0.16	0.00	0.03	0.18	–	–	–	–	–	–	–	–	–
H_2O	–	–	–	–	1.96	1.99	1.97	1.96	12.08	10.93	12.65	–	–	–	–	–	–	–	–	–
Total	99.17	99.47	100.83	101.05	99.61	99.86	99.30	99.55	97.49	97.41	100.32	99.33	99.09	99.05	99.12	99.10	99.02	99.40	99.53	99.19
Si	2.313	2.610	2.896	2.998	6.913	7.609	7.402	7.265	3.137	3.039	3.678	0.004	0.002	0.037	0.003	0.003	0.001	0.003	0.001	0.001
Ti	–	–	–	–	0.236	0.075	0.113	0.135	0.002	0.004	0.001	0.271	0.298	0.424	0.007	0.008	0.037	0.028	0.945	0.947
Al	1.659	1.362	1.101	0.997	1.199	0.450	0.711	0.768	2.048	2.077	1.802	0.075	0.131	0.024	1.351	1.322	0.950	1.007	0.000	0.000
Cr	–	–	–	–	0.000	0.008	0.002	0.004	0.000	0.000	0.001	0.003	0.002	0.002	0.546	0.510	0.805	0.768	0.001	0.001
Fe^{3+}	0.020	0.033	0.010	0.008	–	–	–	–	0.000	0.000	0.000	1.372	1.267	1.052	0.083	0.147	0.170	0.164	0.108	0.104
Fe^{2+}	–	–	–	–	2.867	2.943	2.831	3.065	0.862	2.759	0.848	1.243	1.274	1.425	0.251	0.302	0.406	0.382	0.809	0.916
Mn	–	–	–	–	0.041	0.055	0.044	0.043	0.032	0.022	0.017	0.017	0.018	0.010	0.003	0.003	0.004	0.002	0.126	0.018
Mg	–	–	–	–	2.106	2.525	2.305	2.155	3.694	1.989	3.194	0.003	0.005	0.009	0.755	0.704	0.625	0.630	0.003	0.015
Ca	0.710	0.394	0.076	0.001	1.520	1.246	1.469	1.516	0.034	0.026	0.113	0.013	0.003	0.016	0.001	0.002	0.002	0.015	0.008	0.000
Na	0.285	0.580	0.933	0.990	0.695	0.315	0.470	0.499	0.004	0.002	0.009	–	–	–	–	–	–	–	–	–
K	0.003	0.007	0.002	0.001	0.043	0.033	0.033	0.031	0.000	0.004	0.022	–	–	–	–	–	–	–	–	–
Total	4.991	4.986	5.017	4.995	15.621	15.261	15.381	15.480	9.810	9.921	9.685	3.000	3.000	3.000	3.000	3.000	3.000	3.000	2.000	2.000
An	71.1	40.2	7.5	0.1	–	–	–	–	–	–	–	–	–	–	–	–	–	–	–	–
Mg#	–	–	–	–	42.3	46.2	44.9	41.3	81.1	41.9	79.0	–	–	–	75.0	70.0	60.6	62.3	–	–
Cr#	–	–	–	–	–	–	–	–	–	–	–	3.3	1.5	6.9	28.8	27.9	45.9	43.3	–	–

Formulae calculated on the basis of 8 oxygens and total Fe as trivalent for feldspar; 23 oxygens and fixed number of 15 cations excluding Na and K for amphibole; 14 oxygens and total Fe as divalent for chlorite; 4 oxygens and 3 cations for magnetite-ulvöspinel and chromian spinel; 3 oxygens and 2 cations for ilmenite. Fe_2O_3 is calculated on the basis of fixed number of cations for amphibole, spinels and ilmenite, H_2O corresponds to 2 (OH) and 8 (OH) per formular unit in amphibole and chlorite, respectively. An = 100*Ca/(Ca+Na+K); Mg# = 100*Mg/(Mg+Fe^{2+}), Cr# = 100*Cr/(Cr+Al). c = core, r = rim; MB = massive basalt, PB = pillow basalt; Th = tholeiitic basalt, Alk = alkali basalt.

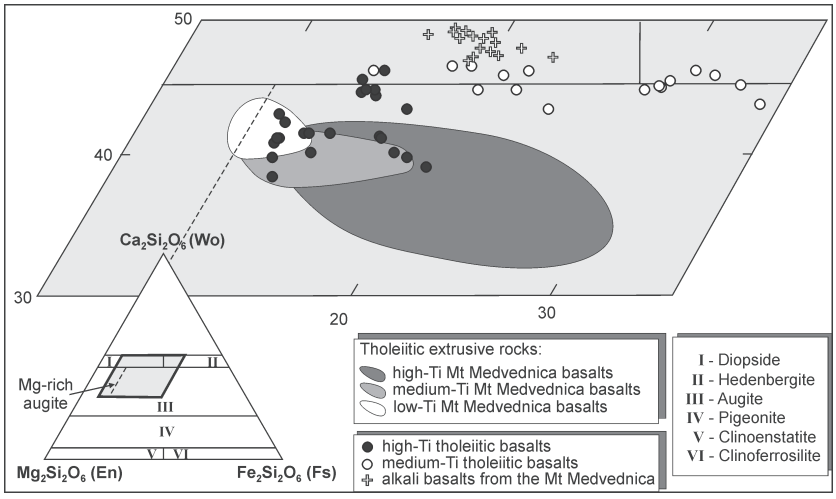

Fig. 3. Plot of clinopyroxene compositions in the En–Wo–Fs ($Mg_2Si_2O_6$–$Ca_2Si_2O_6$–$Fe_2Si_2O_6$) diagram with the nomenclature fields of Morimoto (1988) for tholeiitic volcanic rocks from the Mt Samoborska Gora and alkali volcanic rocks from the Mt Medvednica ophiolite mélange. Fields for clinopyroxene compositions from high-Ti, medium-Ti and low-Ti tholeiitic basalts of the Mt Medvednica ophiolite mélange (Slovenec & Lugović 2008 and 2009) plotted for correlation constraints.

show correlation suggesting significant mobilization during alterations. Large ion lithophile elements (=LILE; Cs, Rb, K, Ba and Sr) represented by Ba in the Ba–Zr plot (Fig. 5A) show highly inconsistent variations which make them unreliable for petrogenetic and discriminatory constraints. High field strength elements (=HFSE; Ti, Th, Hf, Nb, Ta, P, and Y) shown by Ti (Fig. 5B) and rare earth elements (=REE, La-Lu) displayed by La and Sm (Fig. 5C–D) showing good positive correlation with fractionation index have obviously remained immobile. Therefore the HFSE and REE concentrations of our tholeiitic samples may be confidently used to characterize geochemical and petrogenetic features of the rocks as was already successfully tested for similar mafic rocks from different oceanic provenances (e.g. Pearce & Norry 1979; Shervais 1982; Beccaluva et al. 1983). Transitional metals (V, Cr, Mn, Fe, Ni and Zn) represented by Ni and V (Fig. 5E–F) retain magmatic correlation but are strongly related to the abundance and type of the opaque phase hosted in a sample. Similar relations concerning element mobilization are observed in alkali basalts (Fig. 5).

In the Zr/TiO_2 vs. Nb/Y diagram (Winchester & Floyd 1977) frequently used to classify altered and metamorphosed extrusives, the analysed rocks are divided between the fields of subalkali andesite/basalts and alkali basalts, (not shown). Jurassic ophiolitic fragments show exclusively tholeiitic chemistry whilst extrusives associated with Middle Triassic pelagic sediments plot in the field of alkali basalts. Tholeiitic rocks from ophiolite complexes and mélanges are best discriminated by geochemical parameters which include Ti/Cr ratio and Ni concentration (Beccaluva et al. 1983) or simply TiO_2 content (Bortolotti et al. 2002). Following this scheme (not shown) tholeiitic rocks from the Mt Samoborska Gora ophiolite mélange are distinguished into the high-Ti group and medium-Ti group (Table 3). High-Ti basalts are widely accepted as representing crystallization in a middle ocean ridge (=MOR) setting whereas tholeiitic basalts with lower TiO_2 may suggest formation in various suprasubduction zone (=SSZ) settings (Serri 1981; Beccaluva et al. 1983).

Tholeiitic rocks display Ti/V ratios ranging from 21.5 to 44.8 and spread in the field of recent MORB and BABB whereby medium-Ti samples form a separate group with lower V at given Ti (Fig. 6). Alkali basalts from the Mt Samoborska Gora show an increased concentration of Ti at relatively low V (Ti/V=62.2–82.4) and suggest derivation from an enriched mantle source. The referent alkali basalts from the Mt Medvednica with Ti/V ratios of around 50 straggle the boundary line between MORB/BABB and OIB/WPAB.

The element abundance patterns normalized to N-MORB values for analysed extrusive rocks are displayed as spider diagrams in Fig. 7A1 and 7A2. *Tholeiitic rocks* show a wide range of LILE enrichment consistent with the observed alterations. The rock suite displays negative Nb–Ta anomaly relative to La which is typical of SSZ related magmas. The intensity of the anomalies significantly increases from high-Ti group [$(Nb/La)_n$=0.67–0.90] to medium-Ti group [$(Nb/La)_n$=0.32–0.49] suggesting a more subduction influenced nature of the latter. They have nearly flat La–Lu profiles which range from ~1 to ~3 times relative to N-MORB for the high-Ti group and 0.7–1.0 times for the medium-Ti group. A strong to significant positive Sr anomaly in the medium-Ti basalt suggests fractionation of plagioclase. *Alkali basalts* in general show a smooth pattern with typical continuous enrichment of more incompatible elements in the profile from Th to Lu and may show HFSE (P, Nb) positive anomalies. Strong negative anomalies of Ba, K, and Sr are caused by their mobilization due to devitrification and albitization. The alkali basalts from Mt Samoborska Gora are more enriched [$(Th/Lu)_n$=70–85] relative to the Mt Medvednica samples [$(Th/Lu)_n$=32–46]. All samples have Lu_n<1 which may indicate residual garnet in the source. In the spider diagram their profiles, excluding negative anomalies for Ba, K and Sr which are related to alterations, perfectly match the variation patterns of alkali basalts from East African rift zone (Fig. 7A2).

Chondrite normalized REE patterns of analysed rocks are displayed in Fig. 7B1 and 7B2. *Tholeiitic rocks* show various intensities of LREE depletion and nearly flat HREE profile [$(Tb/Lu)_{cn}$=0.96–1.29] at 12–20 times relative to chondrite for the high-Ti group and 10–12 for the medium-Ti group. The intensity of LREE depletion expressed by the ratio $(La/Sm)_{cn}$ increases from the high-Ti group (0.69–0.87) to medium-Ti (0.51–0.62). *Alkali basalts* show strong enrichment of LREE over HREE in the Mt Samoborska Gora samples [$(La/Lu)_{cn}$=9.4–12.8] and relatively lower in the Mt Medvednica samples [$(La/Lu)_{cn}$=6.4–7.6] concordant with relations in the spider diagram (Fig. 7B2). Both groups show slight Eu anom-

Table 2: Selected microprobe analyses and formulae of clinopyroxene from the tholeiitic and alkali volcanic rocks in the Mt Samoborska Gora (SG) and Mt Medvednica (MD) ophiolite mélange.

	SG Tholeiitic High-Ti basalts										SG Tholeiitic Medium-Ti basalts						MD Alkali basalts			
Sample	jf-33/2	jf-33/2	92-20	92-20	92-21	92-21	92-22	92-22	92-30	92-30	js-73/1	js-73/1	js-73/1	js-73/1	jf-23/b2	jf-23/b2	sb-9	sb-9	sb-17	sb-17
Anal. nr.	3	4	30	3	1	2	20	21	16	18	2	16	22	25	13	14	3	4	1	2
Site	c	r	c	r	c	r	c	r	c	c	c	c	c	c	c	r	c	r	c	r
Rock type	PB	PB	MB	MB	MB	MB	PB	PB	MB	MB	MB	MB	MB	MB	PB	PB	MB	MB	PB	PB
SiO_2	48.79	49.10	51.65	50.54	50.91	51.93	52.33	50.51	51.60	52.28	46.85	48.34	47.43	48.68	44.69	45.79	45.65	44.39	47.09	45.65
TiO_2	1.46	1.69	0.55	1.10	0.96	0.65	0.62	0.97	0.70	0.54	2.75	1.78	1.63	1.58	3.05	2.49	3.18	4.17	2.93	3.50
Al_2O_3	5.36	5.51	0.92	2.39	3.00	2.47	1.86	2.15	2.59	1.91	5.34	3.49	5.02	3.92	5.17	4.29	6.72	7.25	6.31	6.20
Cr_2O_3	0.29	0.19	0.01	0.05	0.24	0.12	0.29	0.02	0.45	0.27	0.24	0.05	0.12	0.16	0.26	0.16	0.15	0.10	0.09	0.03
FeO	7.76	8.17	8.64	11.82	8.16	7.28	7.88	10.68	6.87	6.58	12.07	13.77	10.60	11.60	17.38	19.24	9.53	10.37	8.16	11.10
MnO	0.22	0.23	0.35	0.31	0.31	0.21	0.18	0.32	0.21	0.13	0.30	0.41	0.28	0.30	0.40	0.38	0.20	0.19	0.17	0.18
MgO	13.62	13.31	14.03	13.84	15.97	16.23	17.04	14.52	16.42	16.89	10.30	10.80	11.41	11.78	7.40	7.04	11.58	10.75	11.95	10.84
CaO	21.39	21.57	22.90	18.37	19.33	20.00	18.47	19.13	21.11	20.52	21.44	19.92	22.03	20.86	20.40	19.50	21.40	21.84	22.41	21.51
Na_2O	0.39	0.39	0.17	0.39	0.33	0.29	0.22	0.35	0.28	0.30	0.50	0.52	0.49	0.47	0.53	0.55	0.43	0.45	0.41	0.47
Total	99.28	100.17	99.22	98.81	99.20	99.18	98.88	98.64	100.23	99.43	99.79	99.08	99.01	99.36	99.28	99.44	98.84	99.51	99.52	99.49
Si	1.822	1.823	1.941	1.917	1.892	1.925	1.946	1.909	1.892	1.927	1.784	1.857	1.801	1.847	1.751	1.801	1.735	1.687	1.777	1.736
Ti	0.041	0.047	0.015	0.031	0.027	0.018	0.017	0.027	0.019	0.015	0.079	0.051	0.047	0.045	0.090	0.074	0.091	0.119	0.099	0.100
Al^{IV}	0.178	0.181	0.041	0.083	0.107	0.074	0.054	0.091	0.108	0.073	0.216	0.143	0.199	0.153	0.237	0.198	0.265	0.313	0.223	0.264
Al^{VI}	0.058	0.059	0.000	0.024	0.024	0.033	0.027	0.005	0.004	0.010	0.024	0.015	0.026	0.023	0.002	0.001	0.036	0.011	0.057	0.014
Cr	0.009	0.006	0.000	0.002	0.007	0.004	0.008	0.000	0.013	0.008	0.007	0.002	0.004	0.005	0.008	0.005	0.005	0.003	0.003	0.001
Fe^{3+}	0.056	0.042	0.060	0.023	0.047	0.022	0.000	0.055	0.072	0.047	0.064	0.063	0.112	0.070	0.110	0.088	0.073	0.093	0.054	0.083
Fe^{2+}	0.187	0.211	0.212	0.352	0.206	0.203	0.245	0.282	0.138	0.156	0.321	0.379	0.225	0.299	0.459	0.544	0.229	0.237	0.203	0.270
Mn	0.007	0.007	0.011	0.010	0.010	0.007	0.006	0.010	0.007	0.004	0.010	0.013	0.009	0.010	0.013	0.013	0.006	0.006	0.005	0.006
Mg	0.758	0.737	0.786	0.783	0.885	0.897	0.944	0.818	0.892	0.920	0.585	0.618	0.646	0.666	0.432	0.413	0.656	0.609	0.672	0.615
Ca	0.859	0.858	0.922	0.747	0.770	0.794	0.736	0.775	0.829	0.810	0.875	0.820	0.896	0.848	0.857	0.822	0.891	0.889	0.876	0.877
Na	0.026	0.028	0.013	0.029	0.024	0.032	0.016	0.026	0.020	0.021	0.037	0.039	0.036	0.035	0.040	0.042	0.032	0.033	0.030	0.035
Mg#	80.2	77.7	78.8	68.9	80.9	81.5	79.5	74.4	86.68	85.61	64.57	61.99	74.17	69.16	48.49	43.16	74.1	72.0	76.8	69.5
Al^{VI}/Al^{IV}	0.33	0.32	0.00	0.29	0.22	0.44	0.50	0.06	0.04	0.14	0.11	0.10	0.13	0.15	0.01	0.01	0.14	0.04	0.26	0.05

Formulae calculated on the basis of 4 cations and 6 oxygens. MB = massive basalt, PB = pillow basalt, c = core, r = rim. Mg# = 100*Mg/(Mg+Fe^{2+}).

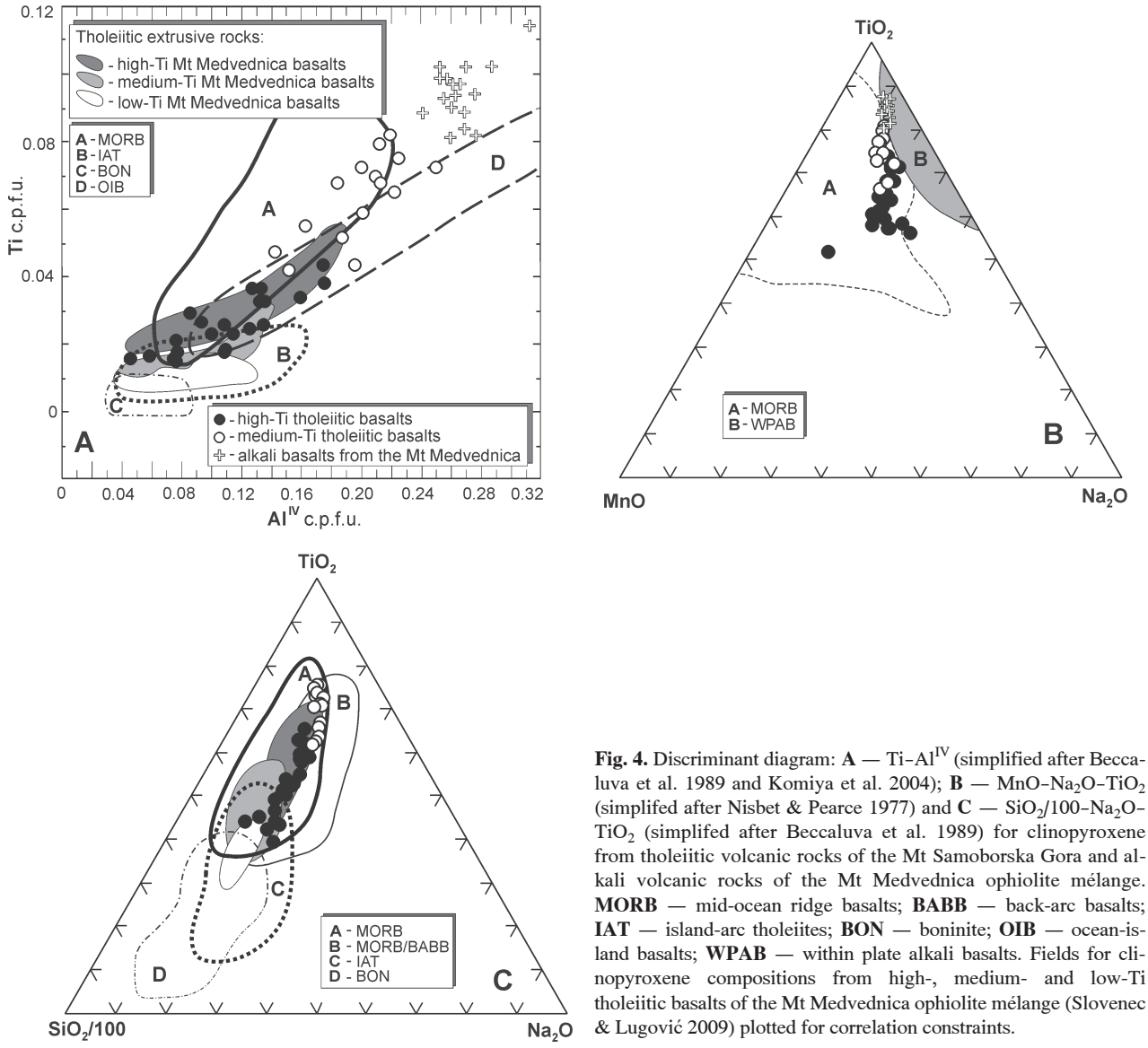

Fig. 4. Discriminant diagram: **A** — Ti–Al^{IV} (simplified after Beccaluva et al. 1989 and Komiya et al. 2004); **B** — MnO–Na_2O–TiO_2 (simplifed after Nisbet & Pearce 1977) and **C** — SiO_2/100–Na_2O–TiO_2 (simplifed after Beccaluva et al. 1989) for clinopyroxene from tholeiitic volcanic rocks of the Mt Samoborska Gora and alkali volcanic rocks of the Mt Medvednica ophiolite mélange. **MORB** — mid-ocean ridge basalts; **BABB** — back-arc basalts; **IAT** — island-arc tholeiites; **BON** — boninite; **OIB** — ocean-island basalts; **WPAB** — within plate alkali basalts. Fields for clinopyroxene compositions from high-, medium- and low-Ti tholeiitic basalts of the Mt Medvednica ophiolite mélange (Slovenec & Lugović 2009) plotted for correlation constraints.

aly (Eu/Eu* = 1.16–0.93) typical for low accumulation or fractionation of plagioclase. The REE paterns of analysed alkali basalts are highly comparable with the profiles of alkali basalts from the East African rift zone (Fig. 7B2).

The Nd and Sr isotopic compositions of two tholeiitic and two alkali basalts are shown in Table 4. In *tholeiitic samples* the $^{143}Nd/^{144}Nd$ ratios are very consistent ranging from 0.512939 to 0.513002 and $^{87}Sr/^{86}Sr$ ratios show a spread between 0.704353 and 0.704422. The initial ε_{Nd} and Sr initial isotopic ratios were calculated for 165 Ma which is assumed as the age of crystallization for the SSZ tholeiitic extrusives of Mt Samoborska Gora ophiolites. The initial ε_{Nd} vary from +6.01 to +6.35 whilst the $(^{87}Sr/^{86}Sr)_i$ ratios vary from 0.703862 to 0.704001. The initial ε_{Nd} and $(^{87}Sr/^{86}Sr)_i$ ratios of the tholeiitic Mt Samoborska Gora mafic extrusives plot in the field of recent back-arc analogues (Fig. 8). In the *alkali basalts* the range of $^{143}Nd/^{144}Nd$ ratios narrows from 0.512602 to 0.512661. The $^{87}Sr/^{86}Sr$ ratios show a spread between 0.705445 and 0.705851. The initial ε_{Nd} and Sr initial isotopic ratios were calculated for 235 Ma (Illyrian–Fassanian) which is assumed as the age of crystallization for alkali basalts of the Mt Samoborska Gora and Mt Medvednica. The initial ε_{Nd} varies between +1.58 to +2.54 whilst the $(^{87}Sr/^{86}Sr)_i$ ratios ranges from 0.705271 to 0.705442. The initial ε_{Nd} and $(^{87}Sr/^{86}Sr)_i$ ratios of both analysed alkali basalts plot in the area of magmas generated from slightly enriched mantle sources bearing Nd-Sr isotopic characteristics close to Bulk Silicate Earth (BSE; Fig. 8).

Discussion

In the Mt Samoborska Gora ophiolite mélange tholeiitic and alkali basalts were geochemically identified. Tholeiitic lavas with N-MORB-like geochemical signatures (high-Ti basalts) and tholeiitic rocks with SSZ characteristics (medium-Ti basalts) are the only ophiolitic lithologies archieved in this mélange which occasionally constitute composite blocks suggesting that diverse ophiolitic lithologies interfere in space

Table 3: Chemical analyses of tholeiitic and alkali volcanic rocks from the Mt Samoborska Gora (SG) and Mt Medvednica (MD) ophiolite mélange.

	SG Tholeiitic High-Ti basalts												SG Tholeiitic Medium-Ti basalts					SG Alkali basalts				MD Alkali basalts			
Sample	jf-33/2	92-20	92-18	92-21	t-56	92-22	92-23	92-30	sas-206	jf-34	js-60	sas-202	t-23b/2	sas-8	t-23b/1	js-73/1	sat-242	sas-203	sas-210	92-16	92-25	sb-9	sb-17	sb-21	sb-30
Rock type	PB	MB	MB	MB	PB	PB	MB	MB	MB	MB	MB	MB	PB	MB	PB	MB	MB	MB	MB	MB	MB	PB	PB	PB	MB
SiO_2	48.57	48.66	49.36	48.96	46.55	49.54	49.97	49.28	46.54	48.59	50.83	49.18	46.98	47.58	46.95	48.01	51.52	54.12	52.32	46.94	55.76	46.66	42.37	47.22	48.63
TiO_2	1.41	1.76	1.79	1.79	1.83	1.88	1.93	1.95	1.96	2.01	2.20	2.31	0.93	0.96	0.97	1.07	1.19	2.57	2.62	2.74	2.70	2.08	1.99	2.08	2.10
Al_2O_3	17.94	14.74	14.71	14.53	15.53	14.55	14.26	14.38	16.13	16.02	19.49	17.74	15.66	16.02	15.27	16.46	17.28	16.30	16.05	15.28	16.15	15.30	15.32	15.28	15.98
$Fe_2O_{3\ total}$	7.48	11.93	12.03	12.05	10.47	12.49	12.71	12.10	12.11	11.04	8.58	13.38	11.63	11.46	11.09	8.69	9.83	10.38	10.04	11.78	9.90	9.09	9.93	9.10	7.39
MnO	0.20	0.19	0.23	0.20	1.24	0.22	0.30	0.27	0.60	0.14	0.11	0.20	0.20	0.21	0.12	0.21	0.69	0.27	0.17	0.31	0.06	0.16	0.15	0.14	0.19
MgO	6.75	6.41	6.83	6.71	4.67	6.41	6.47	6.68	3.94	5.44	4.92	3.77	5.69	5.53	4.35	8.10	3.67	3.17	4.82	8.13	1.08	8.58	8.11	8.07	7.98
CaO	7.97	7.81	7.31	7.02	7.14	7.56	7.21	6.58	4.32	4.26	4.60	2.32	7.87	7.66	8.93	6.88	2.49	1.16	1.92	3.71	1.30	5.03	13.33	7.51	9.62
Na_2O	3.05	4.26	3.85	4.12	4.18	3.98	3.87	4.39	5.88	4.67	4.62	4.51	4.45	4.47	4.59	4.68	6.94	7.03	6.35	5.00	6.41	2.84	1.48	3.21	3.05
K_2O	0.43	0.45	0.50	0.41	0.48	0.37	0.48	0.45	0.32	0.63	0.30	0.57	0.24	0.27	0.21	0.10	0.15	0.68	0.52	0.19	0.68	1.40	0.14	0.38	0.29
P_2O_5	0.15	0.18	0.18	0.17	0.21	0.19	0.19	0.21	0.21	023	0.23	0.24	0.07	0.07	0.09	0.09	0.11	0.82	0.94	0.97	0.93	0.35	0.33	0.39	0.44
LOI	5.69	2.80	3.27	2.93	7.73	2.57	2.93	3.25	7.60	7.12	4.30	5.48	6.16	5.73	7.36	5.58	5.88	3.59	3.56	4.42	4.94	8.46	7.04	6.60	4.26
Total	99.64	99.19	100.06	98.90	100.03	99.76	100.32	99.72	99.69	100.15	100.17	99.70	99.92	100.00	99.83	99.86	99.86	100.09	99.31	99.29	99.91	99.97	99.99	99.98	99.93
Mg#	66.72	54.18	55.54	55.90	48.04	53.04	52.83	55.00	41.25	51.86	55.60	35.89	50.35	49.63	46.27	67.34	44.98	38.56	48.83	60.30	19.39	65.65	64.37	64.25	70.33
Cs	0.5	5.3	2.3	4.7	0.1	1.3	0.8	0.6	0.1	0.4	0.2	0.4	0.3	0.2	0.5	0.1	0.1	0.3	0.2	0.1	0.4	2.0	1.0	1.4	1.6
Rb	13	12	14	12	5	9	13	11	3	9	3	4	7	5	16	2	2	25	21	3	39	6	10	43	41
Ba	268	1070	1270	737	81	631	273	258	77	240	47	80	62	69	233	78	85	83	71	74	60	79	30	74	49
Th	0.28	0.45	0.46	0.41	0.60	0.45	0.47	0.60	0.43	0.61	0.32	0.49	0.06	0.07	0.07	0.07	0.09	7.05	7.14	6.60	7.79	3.69	2.70	3.98	4.12
Ta	0.14	0.33	0.32	0.28	0.30	0.27	0.26	0.31	0.22	0.23	0.22	0.21	0.04	0.05	0.04	0.04	0.06	3.88	3.93	3.68	4.02	2.10	1.91	2.31	2.42
Nb	2.2	5.4	5.2	4.5	4.9	4.5	4.5	4.7	3.4	3.6	3.4	3.3	0.6	0.8	0.7	0.7	1.0	60.3	60.7	58.2	62.6	33.9	30.8	35.2	38.7
Sr	142	301	415	307	175	369	307	264	63	109	162	90	719	711	308	1407	98	85	72	167	58	139	70	92	103
Zr	89	116	122	122	115	134	141	132	141	140	135	151	47	49	50	69	59	245	251	255	274	152	147	168	173
Hf	2.4	3.5	3.6	3.5	3.5	3.9	4.1	3.6	3.7	3.9	4.0	4.0	1.5	1.4	1.6	1.8	1.7	6.1	6.2	6.3	6.8	3.5	3.5	3.8	3.9
Y	30	34	36	35	36	37	39	44	38	34	35	33	28	28	26	27	24	36	34	30	35	29	27	31	33
Sc	33	37	36	34	46	35	36	37	41	40	36	33	43	45	43	43	45	19	17	23	13	31	29	32	32
V	230	2.88	283	279	245	289	301	355	315	382	406	414	256	269	234	221	211	238	241	268	196	261	254	251	245
Cr	430	213	177	152	226	100	98	115	410	190	120	145	384	460	233	470	440	80	92	271	20	239	301	292	252
Co	46	-	-	-	33	-	-	39	43	38	72	42	58	61	57	57	64	35	29	-	23	36	43	34	31
Ni	140	70	60	53	56	50	47	41	140	50	45	42	265	270	182	260	290	32	39	117	20	146	230	152	122
La	3.21	6.41	6.64	6.29	4.09	6.83	7.21	6.37	4.53	5.12	4.73	3.92	1.62	1.80	1.71	2.35	2.19	32.71	33.41	43.91	31.40	21.21	19.72	22.25	24.86
Ce	10.18	17.90	18.51	18.10	13.03	19.32	20.60	18.8	14.20	15.11	14.40	12.21	5.34	5.75	5.55	7.79	6.91	69.10	70.33	97.82	67.11	47.79	45.13	49.32	54.98
Pr	1.62	2.80	2.87	2.79	1.98	2.98	3.14	2.78	2.15	2.23	2.24	1.88	0.91	0.95	0.90	1.34	1.12	8.33	8.24	12.10	7.44	5.29	5.04	5.62	6.22
Nd	8.89	14.60	15.11	15.22	10.92	16.31	17.10	14.52	12.20	12.21	12.01	10.20	5.30	5.62	5.20	7.56	6.12	32.22	33.15	47.71	31.21	22.81	21.41	23.99	25.99
Sm	2.92	4.79	4.96	4.74	3.36	5.16	5.35	4.62	4.21	3.84	3.67	3.22	2.00	2.06	2.00	2.59	2.23	7.03	7.62	9.52	6.51	4.79	4.59	4.99	5.32
Eu	1.21	1.71	1.78	1.74	1.33	1.83	1.89	1.80	1.49	1.45	1.41	1.31	0.88	0.97	0.82	1.14	0.94	2.22	2.26	3.01	2.12	1.61	1.64	1.75	1.87
Gd	3.83	5.77	5.88	5.78	4.39	6.20	6.36	6.08	5.35	4.88	4.75	4.28	3.40	3.50	3.15	3.49	3.19	6.83	6.99	7.99	6.23	4.92	4.70	5.13	5.39
Tb	0.79	1.11	1.12	1.09	0.85	1.12	1.20	1.18	1.00	0.98	0.91	0.84	0.66	0.70	0.64	0.72	0.59	1.15	1.19	1.99	1.10	0.89	0.88	0.93	0.95
Dy	4.96	7.06	7.06	7.05	5.47	7.42	7.67	7.58	6.36	6.31	6.07	5.50	4.10	4.72	4.00	4.70	3.79	6.40	6.42	6.21	6.34	4.79	4.65	5.10	5.29
Ho	1.12	1.42	1.47	1.45	1.24	1.54	1.63	1.56	1.32	1.27	1.32	1.19	0.98	1.02	0.93	0.97	0.88	1.21	1.24	1.18	1.15	1.01	0.97	1.07	1.10
Er	3.22	4.53	4.57	4.49	3.55	4.75	5.03	4.72	3.99	3.75	4.18	3.68	2.97	3.15	2.71	2.94	2.59	3.22	3.27	3.27	3.13	2.76	2.64	2.84	2.88
Tm	0.493	0.661	0.668	0.667	0.541	0.703	0.741	0.699	0.592	0.562	0.636	0.554	0.441	0.472	0.413	0.426	0.399	0.437	0.439	0.442	0.426	0.382	0.371	0.390	0.393
Yb	3.13	3.97	3.98	4.09	3.50	4.23	4.46	4.39	3.88	3.59	4.10	3.42	2.95	2.90	2.55	2.75	2.50	2.58	2.59	2.56	2.53	2.46	2.35	2.49	2.52
Lu	0.482	0.558	0.567	0.572	0.482	0.594	0.634	0.666	0.606	0.538	0.615	0.504	0.452	0.461	0.401	0.416	0.383	0.359	0.361	0.355	0.347	0.331	0.321	0.338	0.342

Major elements in wt. %, trace elements in ppm. LOI = loss on ignition at 1100 °C. PB = pillow basalt; MB = massive basalt. Mg# = 100 * molar ($MgO/(MgO+FeO_{total})$).

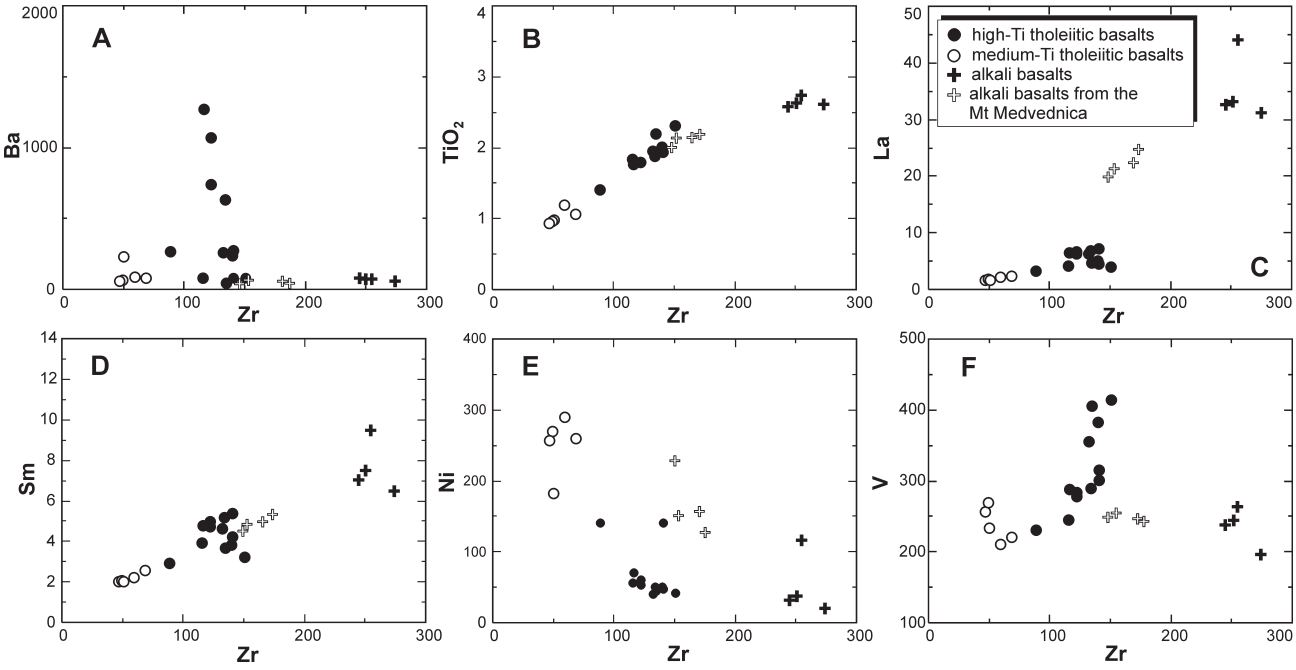

Fig. 5. Variation diagrams for selected elements with Zr as index of fractionation for the tholeiitic and alkali volcanic rocks from the Mt Samoborska Gora and alkali volcanic rocks from the Mt Medvednica ophiolite mélange.

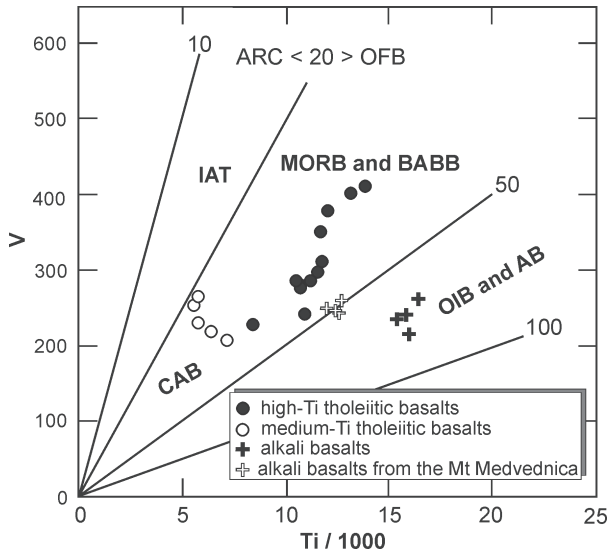

Fig. 6. V–Ti/1000 discrimination diagram (Shervais 1982) for the tholeiitic and alkali volcanic rocks from the Mt Samoborska Gora and alkali volcanic rocks from the Mt Medvednica ophiolite mélange. **IAT** — island-arc tholeiites, **MORB** — mid-ocean ridge basalts, **BABB** — back-arc basin basalts, **CAB** — calc-alkaline basalts, **CFB** — continental flood basalts, **OIB** — ocean-island basalts and **AB** — alkali basalts.

and time. Thus the studied rocks from the Mt Samoborska Gora ophiolite mélange contribute to the ophiolite controversy: how rocks, which have been formed in different tectonomagmatic settings (e.g. Western and Eastern Albanian ophiolites, Dinaric and Vardar ophiolites, etc.), come together in a small regional scale lacking any *tectonic* contact. In an ophiolite mélange various sequences of the oceanic crust which are unrelated in the term of time and crystallization setting may be found juxtaposed in the finally formed mélange (see detail study of Saccani & Photiades (2005) for Albanian ophiolite mélanges). Materials detached from the oceanic lithosphere, which are incorporated in an ophiolite mélange, record polyphase history of formation which includes a variety of sedimentary and tectonic processes during deposition in an accretionary wedge and subsequent tectonic incorporation through onset of thrusting and final emplacement onto a passive continental margin. The Mt Samoborska Gora ophiolite mélange closely exposes Middle Triassic non-orogenic alkali basalts and different tholeiitic extrusives, some of them showing uppermost Bathonian–Early Callovian age, which may facilitate the study of evolution of the oceanic domain where these ophiolites were formed from the initial stage of opening till the initiation of shortening of the oceanic domain.

Tectonomagmatic significance of tholeiitic basalts

The extrusive rocks archived in the Mt Samoborska Gora ophiolite mélange show geochemical signatures that reflect magmas derived from several parental mantle sources which are obviously related to the different tectonomagmatic settings (Pearce & Norry 1979; Pearce 1983). Composite blocks of tholeiitic extrusives suggest that the high-Ti and medium-Ti magmatism may be temporally and spatially closely interrelated. Similar overlaping of contrasting magma types seems to be very common in Neotethyan ophiolites as exemplared by the Mirdita ophiolites in Albania (Bébien et al. 2000; Hoeck et al. 2002; Bortolotti et al. 2002; Dilek et al. 2007).

The high-Ti and medium-Ti basalts from the Mt Samoborska Gora ophiolite mélange show N-MORB-like REE patterns

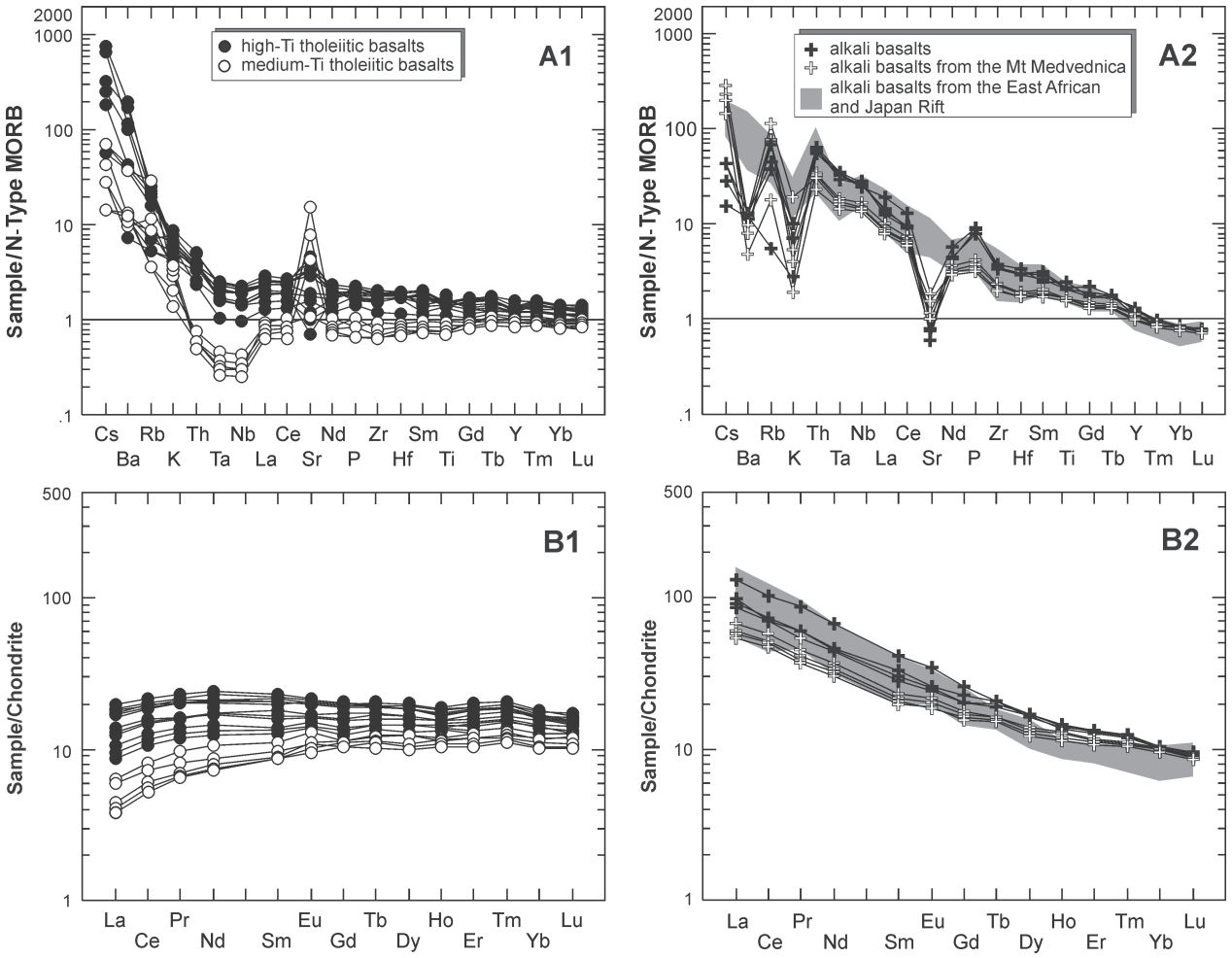

Fig. 7. N-MORB-normalized **(A)** multielement and **(B)** REE patterns for tholeiitic and alkali volcanic rocks from the Mt Samoborska Gora and alkali volcanic rocks from the Mt Medvednica ophiolite mélange. Field for alkali basalts from the East African Rift-Kenya Rift (Wilson 1989 and references therein; Spath et al. 2001) and Japan Rift (Okamura et al. 2005) are shown for comparision. Normalization values are from Sun & McDonough (1989).

(Fig. 7B1) and at the same time show HFSE negative anomalies (Fig. 7A1) which are unique characteristics of MORBs with arc signatures (Shervais 2001). Surprisingly, although the LREE depletion in the medium-Ti basalts is more pronounced they display considerably higher relative depletion of Ta–Nb thus confronting MORB and SSZ signatures in one single geochemical group. In the diagram V-Ti/1000 all tholeiitic basalts from the Mt Samoborska Gora plot in the field of ocean ridge basalts (Fig. 6). However, they may plot between the fields of MORB and IAT extrusives forming a SSZ array similar to the recent back-arc basin basalts (Fig. 9A–C). The Nd isotopic composition of the tholeiitic rocks from the Mt Samoborska Gora ophiolite mélange expressed in the term of $\varepsilon_{Nd(T=165\ Ma)}$ shows vary small range from +6.01 in the high-Ti basalts to +6.35 in medium-Ti basalts and strongly suggests that medium-Ti basalts must have derived from a similar but slightly more depleted mantle source during the second stage of partial melting. Combined with initial $^{87}Sr/^{86}Sr$ ratios ranging from 0.703862 to 0.704001, respectively (Table 4), the tholeiitic rocks better match BABB then N-MORB (Fig. 8).

Clinopyroxene chemistry is frequently used to discriminate and characterize the tectonomagmatic setting of parental basalts (Beccaluva et al. 1980; Pearce & Wanming 1988; Pearce 2003). Beccaluva et al. (1989) promote clinopyroxene composition as a robust discriminator for host basalts from different ophiolitic types. The composition of clinopyroxenes from the Mt Samoborska Gora ophiolite mélange clearly discriminate tholeiitic basalt host rocks in the fields of MORB and BABB (Fig. 4A–C). Clinopyroxenes hosted in the medium-Ti samples plot at high-Ti corner of the MORB/BABB field (Fig. 4A and 4C), although following the petrochemical parameters of this discriminatory concept, they should plot between the MORB/BABB and IAT fields. The clinopyroxene from our medium-Ti basalts exceptionally coexists with abundant *spinel* and minor *Ti-magnetite*. The significantly higher partition of Ti in clinopyroxene compared with coexisting spinel in a tholeiitic melt, cause clinopyroxene to become enriched in Ti and also in Fe (Figs. 3 and 4), which is generally atypical for clinopyroxenes hosted in ophiolitic medium-Ti and low-Ti basalts (e.g. Bortolotti et al. 2002; Slovenec & Lugović 2009). Due to lower partition of Ti in spinel relative to Fe-Ti

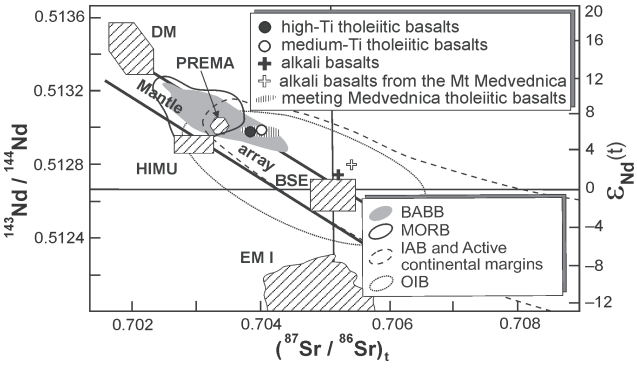

Fig. 8. Initial $^{143}Nd/^{144}Nd$–$^{87}Sr/^{86}Sr$ isotope ratios diagram for selected high-, and medium-Ti tholeiitic rocks from the Mt Samoborska Gora (time: 165 Ma) and alkali extrusive rocks from the Mts Samoborska Gora and Medvednica (time: 235 Ma) ophiolite mélange showing the main oceanic mantle reservoirs of Zindler & Hart (1986). Fields for the Mt Medvednica tholeiitic basalts (Slovenec & Lugović 2009) plotted for correlation constraints. **DM** — depleted mantle, **BSE** — bulk silicate Earth, **EMI** — enriched mantle, **HIMU** — mantle with high U/Pb ratio, **PREMA** — frequently observed PREvalent MAntle composition. The mantle array is defined by many oceanic basalts and a bulk Earth value for $^{87}Sr/^{86}Sr$ can be obtained from this trend. Data for back-arc basin basalts — BABB (shaded field) compiled from Wilson (1989) and references therein, Cousens et al. (1994) and references therein, Pearce et al. (1995), Gribble et al. (1998) and Ewart et al. (1998). Data for mid-ocean ridge basalts — **MORB** (solid line) compiled from Wilson (1989) and references therein and Cousens et al. (1994), references therein and Peate et al. (1997). Data for oceanic island arcs and active continental margins — **IAB** (broken line) compiled from Wilson (1989) and references therein, Cousens et al. (1994) and references therein, Pearce et al. (1995) and Peate et al. (1997).

oxide(s), caution is recommended concerning liability of clinopyroxene in paragenesis with spinel as a tectonomagmatic discriminatory tool.

Coexistence of the high-Ti and medium-Ti basalts in the ophiolite mélange of the Mt Samoborska Gora suggests at least two stages of partial melting and magma generation: an older stage producing crust with N-MORB-like geochemical signatures at an ocean spreading ridge *closely* followed by the stage marked by formation of the younger crust which involves subduction related melt. The high-Ti group from the Mt Samoborska Gora ophiolite mélange derived from a mantle source and experienced low total partial melting ranging from <5 to 10 % (Fig. 10A), leaving residual fertile mantle peridotites closely resembling the composition of the lherzolites from the Mt Kalnik (Lugović et al. 2007) and from the entire CDOB (Lugović et al. 1991; Bazylev et al. 2009). This geochemical group is accepted as representing remnants of the crust formed at the ocean ridge at any time in the ocean's spreading history.

On the contrary, the Upper Bathonian–Lower Callovian high-Ti basalts, crystallized at around 165 Ma, that are associated with the medium-Ti basalts in the composite block, indicate terminal formation of high-Ti crust which may be related to *subducting ridge* and indicate incipient crust formation in the hanging wall or, in other words, in the upper plate. These composite blocks give strong evidence for the "stage of birth" from the geodynamic model of SSZ ophiolites proposed by Shervais (2001). Stern (2004) thought that such association of extrusive rocks were formed by extensive magmatism in the extensional proto-arc–fore-arc basin that spreads over the still active subducting ridge. Extension in the proto-arc or infant-arc basin lasts 5–10 Ma and is normally marked by almost simultaneous crystallization of high-Ti and medium-Ti to low-Ti basalts as a consequence of melt derivation from successively more depleted mantle which was progressively more metasomatized by expulsion of fluids from the subducting slab.

Since the high-Ti basalts from ocean spreading center and from proto-arc–fore-arc extensional basin were derived from essentially similar sources they are geochemically hardly distinguishable. Following the proposed geodynamic models, the medium-Ti basalts from Mt Samoborska Gora ophiolite mélange showing significantly higher HFSE depletion (Fig. 7A1) and Nd isotopic composition (Table 4) clearly resemble magmatism of the second stage partial melting from an already moderately depleted mantle source contaminated by an amount of subduction related components. Here, the second stage melting is somewhat atypical since it allows cotectic crystallization of clinopyroxene and spinel±Ti-magnetite instead of ordinary Fe-Ti oxide(s) as recorded in analogue rocks from ophiolite mélanges included in the nearby Kalnik Unit. This may suggest a different thermal regime governing incipi-

Table 4: Nd and Sr isotope data of tholeiitic and alkali volcanic rocks from the Mt Samoborska Gora and Mt Medvednica ophiolite mélange.

Sample	Location	Rock type	$^{143}Nd/^{144}Nd$ [a]	$^{147}Sm/^{144}Nd$	$^{87}Sr/^{86}Sr$ [a]	$\varepsilon_{Nd(t)}$ [b]	$^{87}Sr/^{86}Sr_{(t)}$ [c]
jf-34	2	Th, H-Ti, MB	0.512939 (4)	0.19015	0.704422 (12)	+6.01*	0.703862*
t-23B/1	2	Th, M-Ti, PB	0.513002 (9)	0.23255	0.704353 (11)	+6.35*	0.704001*
92-16	13	Alk, MB	0.512602 (15)	0.12063	0.705445 (9)	+1.58*	0.705271*
sb-9	MD	Alk, PB	0.512661 (7)	0.12696	0.705851 (14)	+2.54*	0.705442*

Location number corresponds to the locations in Fig. 1C for the samples from the Mt Samoborska Gora; MD = Mt Medvednica. Rock types: Th = tholeiitic, Alk = alkali, H-Ti = high-Ti, M-Ti = medium-Ti, PB = pillow basalt, MB = massive basalt. [a] Errors in brackets for Nd and Sr isotopic ratios are given at the 2σ-level. $^{147}Sm/^{144}Nd$ calculated from the ICP-MS concentrations of Sm and Nd following equation: $^{147}Sm/^{144}Nd = (Sm/Nd)*[0.53151+0.14252*^{143}Sm/^{144}Nd]$. [b] Initial $\varepsilon_{Nd(t)}$ calculated assuming $I^{o}_{CHUR} = 0.512638$, $(^{147}Sm/^{144}Nd)^{o}_{CHUR} = 0.1966$, and $\lambda_{Sm} = 6.54*10^{-12}$ a^{-1}. [c] $^{87}Sr/^{86}Sr_{(t)}$ calculated using ICP-MS Rb and Sr concentrations and assuming $\lambda_{Rb} = 1.42*10^{-11}$ a^{-1}. * The initial ε_{Nd} and initial isotopic ratios for Sr in analysed tholeiitic (Th) rocks are calculated for 165 Ma, and in alkali (Alk) rocks are calculated for 235 Ma.

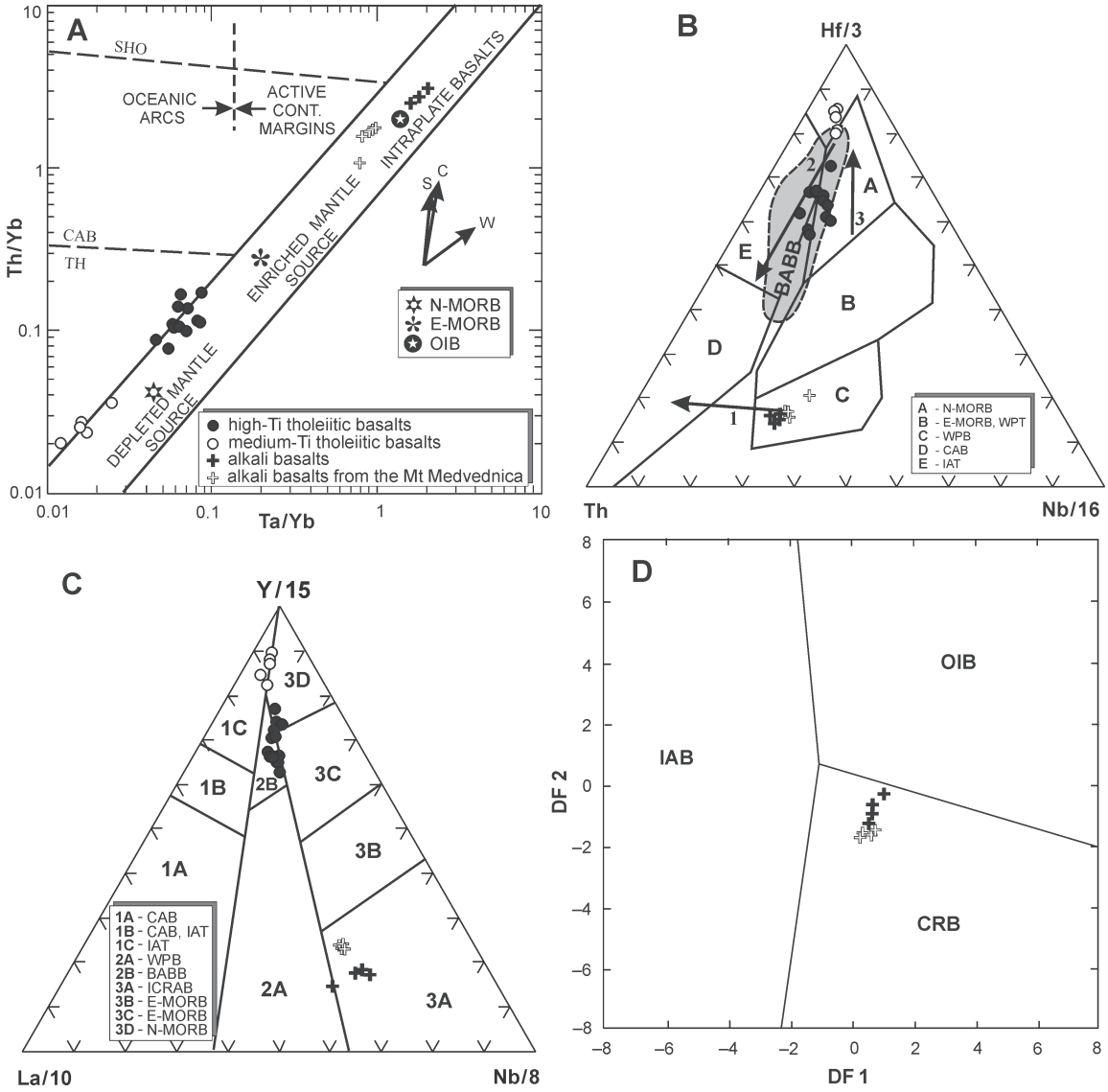

Fig. 9. Discrimination diagrams for the tholeiitic and alkali volcanic rocks from the Mt Samoborska Gora and alkali vocanic rocks from the Mt Medvednica ophiolite mélange. **A** — Ta/Yb–Th/Yb diagram (Pearce 1983); S — subduction zone enrichment, C — crustal contamination, W — within-plate enrichment. N-MORB, E-MORB and OIB are from Sun & McDonough (1989). **B** — Th–Nb/16–Hf/3 diagram (Wood 1980); A — normal mid-ocean ridge basalts (N-MORB), B — enriched MORB (E-MORB) and within-plate tholeiites (WPT), C — alkaline within-plate basalts (AWPB), D — calc-alkali basalts (CAB), E — island-arc tholeiites (IAT); 1 — crustal contamination, 2 — SSZ ophiolites trend, 3 — MORB ophiolites trend. Data for back-arc basin basalts — BABB (shaded field) compiled from Saunders & Tarney (1979), Weaver et al. (1979), Crawford & Keays (1987), Jahn (1986), Ikeda & Yuasa (1989), Ewart et al. (1994), Gribble et al. (1998), Leat et al. (2000), Münker (2000). **C** — La/10–Nb/8–Y/15 diagram (after Cabanis & Lecolle 1989); 1A — calc-alkali basalts (CAB), 1B — area of overlap between 1A and 1C (CAB, IAT), 1C — island-arc tholeiites (IAT), 2A — within plate basalts (WPB), 2B — back-arc basin basalts (BABB), 3A — intercontinental rift alkali basalts (ICRAB), 3B — enriched mid-ocean ridge basalts (E-MORB), 3C — weakly enriched mid-ocean ridge basalts (E-MORB), 3D — normal mid-ocean ridge basalts (N-MORB). **D** — DF_1–DF_2 diagram (Agrawal et al. 2008; $DF_1 = 0.5533\log_e (La/Th) + 0.2173\log_e (Sm/Th) - 0.0969\log_e (Yb/Th) + 2.0454\log_e (Nb/Th) - 5.6305$; $DF_2 = -2.4498\log_e (La/Th) + 4.8562\log_e (Sm/Th) - 2.1240\log_e (Yb/Th) - 0.1567\log_e (Nb/Th) + 0.94$). IAB — island-arc basalts, OIB — ocean-island basalts, CRB — continental rift basalts.

ent crust formation in the upper plate of the oceanic segment represented by the Mt Samoborska Gora ophiolite mélange. The medium-Ti basalt derived from a metasomatized mantle region experienced 13–22 % total partial melting (Fig. 10A). Transitional harzburgites, tectonically inserted into the Campanian-Maastrichtian rudist limestones near the village of Gornje Orešje in the Mt Medvednica (Lugović et al. 2007), showing ~20 % partial melt extraction probably represent the most depleted residual mantle from which the medium-Ti basalts from Mt Samoborska Gora were derived.

Tectonomagmatic significance of alkali basalts

Alkali basalts are very commonly associated with tholeiitic rocks in many Mesozoic ophiolite mélanges and were mostly interpreted as remnants of intraoceanic islands (OIB) or sea-

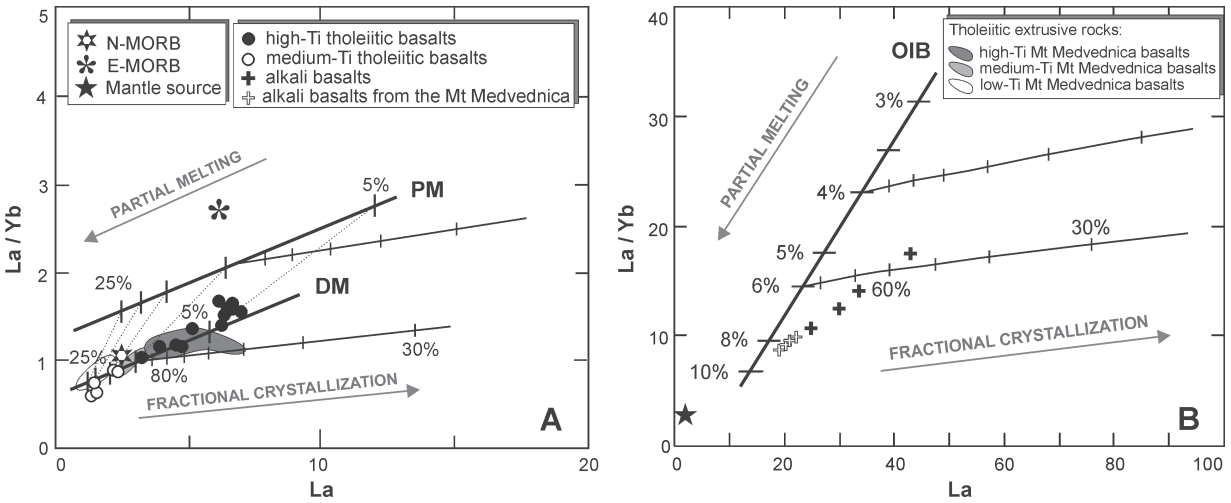

Fig. 10. Petrogenic model for: **A** — mafic tholeiitic volcanic rocks from the Mt Samoborska Gora ophiolite mélange. Partial melting lines: DM — depleted mantle source, PM — primitive mantle source (Kostopoulos & James 1992). Model parameters = spinel-lherzolite source (ol_{57}-$opx_{25.5}$-cpx_{15}-$sp_{2.5}$), melting proportion = $ol_{1.21}$-$opx_{8.06}$-$cpx_{76.37}$-$sp_{14.36}$, distribution coefficients are from Kostopoulos & James (1992). Fractional crystallization lines: initial magma = 10% melting of DM and PM mantle source, respectively, fractionated mineral assemblage = ol_{30}-cpx_{40}-pl_{30}, distribution coefficients are from Chen et al. (1990). Data for N-MORB, E-MORB are from Sun & McDonough (1989). Fields for high-, medium- and low-Ti tholeiitic basalts from the Mt Medvednica ophiolite mélange (Slovenec & Lugović 2009) plotted for correlation constraints. **B** — mafic alkali volcanic rocks from the Mt Samoborska Gora and Mt Medvednica ophiolite mélange. Partial melting lines: moderately enriched mantle source (OIB-like) (La = 1.5 ppm, Yb = 0.5 ppm). Model parameters = garnet-lherzolite source ($ol_{60.1}$-$opx_{18.9}$-$cpx_{13.7}$-$gt_{7.3}$), melting proportion = $ol_{1.3}$-$opx_{8.7}$-cpx_{36}-gt_{54}, distribution coefficients are from Kostopoulos & James (1992). Fractional crystallization lines: initial magma = 4% and 6% melting of the moderately enriched mantle source, fractionated mineral assemblage = ol_{30}-cpx_{40}-pl_{30}, distribution coefficients are from Chen et al. (1990).

mounts (Saccani & Photiades 2005; Monjoie et al. 2008; Sayit & Göncüoglu 2009). However, alkali basalts from continental rifts (=CRB) closely preceding formation of early oceanic crust as a rule have a similar composition (e.g. Fitton 2007) which discriminates them as within-plate volcanic rocks (Fig. 9B). We do not exclude either OIB or CRB origin of alkali basalt fragments incorporated in the Mts Samoborska Gora and Medvednica ophiolite mélanges.

Although alkali basalts from the Mts Samoborska Gora and Medvednica ophiolite mélanges in general share geochemical characteristics of OIB and CRB, they show slightly pronounced geochemical differences (Fig. 7A2, 7B2) suggesting a more enriched or less depleted source for the Mt Samoborska Gora alkali basalts (Figs. 6, 9A). Low relative abundance of HREE in these alkali basalts suggests presence of garnet as a residual phase in both sources (e.g. Wilson 1989; Spath et al. 1996).

Crustal contamination of alkali basalts increases the LILE or LREE/HFSE ratios, with higher intensity in CRB than in OIB. Uncontaminated CRB have La/Ta ratio <22 (e.g. Fitton et al. 1988; Hart et al. 1989) and the ratio of the analysed alkali basalts is even lower (7.8–11.9) suggesting insignificant crustal contamination. Therefore the analysed alkali basalts represent uncontaminated melts and plot in the field of mantle array in the diagram Th/Yb–Ta/Yb wherein alkali basalts from the Mt Samoborska Gora also show a more primitive nature (Fig. 9A). Many attempts based on geochemical parameters were done to discriminate between OIB and CRBs. Recent multielement ratios discriminate function analysis resolve CRB and OIB in two separate fields at 78% and 85% confidence level, respectively (Agrawal et al. 2008). Alkali basalts from the Mts Samoborska Gora and Medvednica mélanges show overall geochemical signatures comparable with CRB (Fig. 9D). Thus, the alkali basalts are interpreted as the pre-ophiolitic continental rift basin volcanic rocks, rather than as the remnants of intraoceanic islands or seamounts.

Continental intraplate alkali basalts were interpreted as volcanic products of partial melting of the upper mantle related to lithospheric extension causing upwelling of the asthenosphere (Perry et al. 1990; Kent et al. 1992). Alternatively, alkali basalts may erupt when the mantle plume impinges on the base of the continental lithosphere causing partial melting and initial rifting (Morgan 1981; McKenzie & Bickle 1988). The analysed alkali basalts reflect melt derived from an OIB-type enriched mantle source (Fig. 9A), which experienced ~8% total partial melting for the Mt Medvednica and 5–7% for the Mt Samoborska Gora (Fig. 10B). Assuming that both groups of the alkali basalts were derived from the same or similar parental asthenospheric material, which resembles Nd-Sr isotopic signatures of the bulk Earth at the time of crystallization (Fig. 8), then the alkali basalts from the Mt Samoborska Gora with more primitive geochemical significance, particularly lower $\varepsilon_{Nd(T=235\ Ma)}$ (+1.58 vs. +2.54; Table 4) represents melts of an older stage of partial melting. If this assesment is correct, Illyrian-Fassanian age is promoted as the age of initial Neotethyan opening in the ROD.

Geodynamic evolution of the Mt Samoborska Gora ophiolites in the context of the Repno oceanic domain

The ophiolite mélange of the Mt Samoborska Gora is tectonically emplaced directly on the Adria amagmatic continental margin and represents the southwesternmost detached

leading edge of a larger ophiolite mélange unit, most likely of the Kalnik Unit (Haas et al. 2000) from the Zagorje-Mid-Transdanubian Zone (Fig. 1A,B). The tectonomagmatic history of the Kalnik Unit has been in part successfully inferred from the remnants of the oceanic upper crustal rocks archived in the Mt Medvednica ophiolite mélange (Slovenec & Lugović 2008, 2009) thought to have been generated in a discrete Neotethyan oceanic domain referred to as the Repno oceanic domain (ROD) (Babić et al 2002; Slovenec & Lugović 2008). The ROD should be included in easternmost segment of the Tethys (Bortolotti & Principi 2005). Some authors regard the ROD as a domain of Dinaric provenance (e.g. Pamić 1997; Haas & Kovács 2001) whilst others relate it to the Meliata-Maliac ocean system (e.g. Goričan et al. 2005; Slovenec & Lugović 2008). These basins opened as back-arc basins in response to the delayed subduction of the Paleotethyan lithosphere beneath the European continental margin (Stampfli & Borel 2002, 2004).

The geochemical affinities and age of crystallization of analogous ophiolitic rocks from the Mt Samoborska Gora ophiolite mélange and the Mt Medvednica segment of the Kalnik Unit were used for correlation of these two ophiolitic segments. Normalized multi-element concentration (Fig. 11A), normalized REE concentrations (Fig. 11B) and Nd and Sr isotopic signatures (Fig. 8) of the analogue high-Ti N-MORB-like extrusives from both ophiolitic segments, assumed to represent the oceanic crust formed at a spreading or subducting ridge, show identical patterns suggesting a similar mantle source. The high-Ti basalts from the composite blocks in Mts Samoborska Gora and Medvednica ophiolite mélanges, which indicate incipient crust formation in a converging upper plate, show identical K-Ar ages of 165.4±5.8 Ma and 165.1±3.3 Ma, respectively. The medium-Ti extrusives which represent relatively younger incipient crust for Mt Samoborska Gora show more pronounced subduction signatures (Fig. 11A) and different crystallization regime as revealed by paragenesis of clinopyroxene and spinel (Figs. 3 and 4A,C), and reveal a higher intensity of partial melting (Fig. 10A). However, inspite of this, the Mt Samoborska Gora lacks the fragments of typical IAT-like lithologies (low-Ti basalts) that are related to the early stage of true subduction sensu Stern (2004). This may suggest that the Mt Samoborska Gora ophiolites represent a discrete segment at the stage of incipient intraoceanic convergence. The overlapping of geochemical signatures and age of crystallization of analogue rocks from these two ophiolite mélange sectors allow them to be integrated into a single ophiolite mélange unit, namely the Kalnik Unit. This finding will serve to improve the geodynamic evolution of the ROD that was already proposed by Slovenec & Lugović (2009). In this respect, the newly discovered alkali basalts play a key role for initiation of the ROD.

(1) Incipient opening of the ROD most likely started in the Early Ladinian, namely in the Fassanian, soon after the eruption of the alkali basalt during the Illyrian–Fassanian (Fig. 12A). This stage is documented by the close association of alkali basalts with Middle Triassic cherts in the Mt Samoborska Gora and interpillow Illyrian–Fassanian pelagic limestones in the Mt Medvednica, and also by the absence of any crustal contamination of the alkali lavas, suggesting their effusion in a highly evolved intracontinental rift basin. These statements are also confirmed by similar geochemical patterns with intracontinental alkali basalts from East African rift zone (Fig. 7A2, 7B2).

(2) The onset of oceanic crust formation at ensialic BAB spreading centre in the ROD continued through the Carnian (Fig. 12B) as documented by radiolarians cherts above the pillow lavas (Halamić & Goričan 1995; Goričan et al. 2005). The fragments of the early oceanic crust of the ROD were not encountered elsewhere in the Kalnik Unit. The oceanic crust formation recorded in Eastern Mediterranean ophiolites, such as

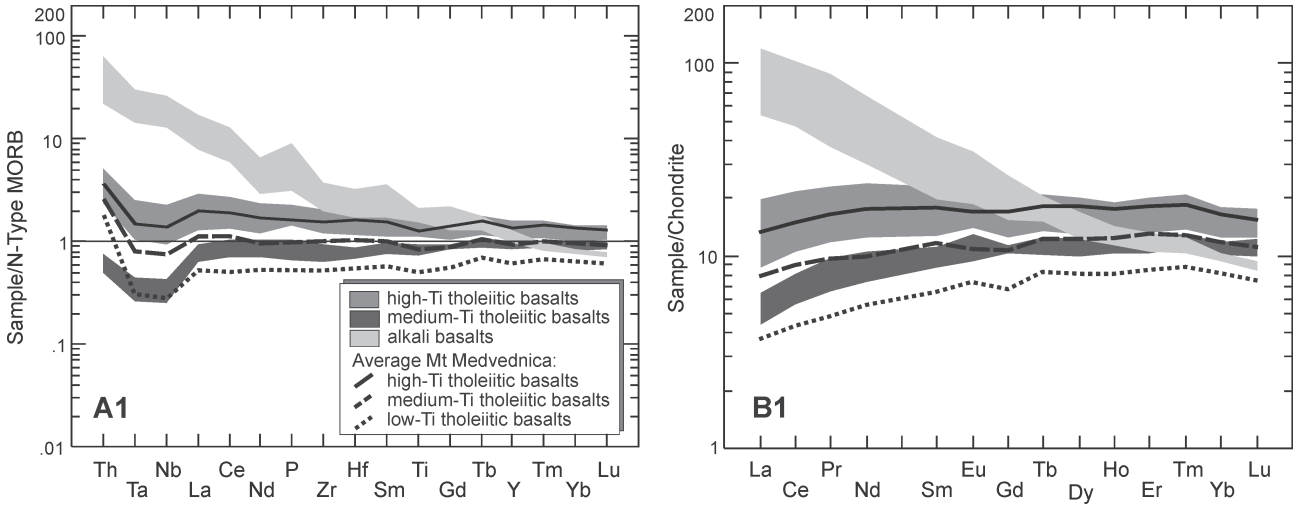

Fig. 11. (A) N-MORB-normalized multielement patterns and **(B)** chondrite-normalized REE patterns for average high-, medium- and low-Ti tholeiitic basalts from the Mt Medvednica ophiolite mélange. Fields for tholeiitic high- and medium-Ti basalts and alkali basalts from the Mts Samoborska Gora and Medvednica ophiolite mélange are shown for comparision. Data for the Mt Medvednica tholeiitic high-, medium- and low-Ti basalts from Slovenec & Lugović (2009). N-MORB normalization values are from Sun & McDonough (1989), and Chondrite normalization values are from Taylor & McLennan (1985).

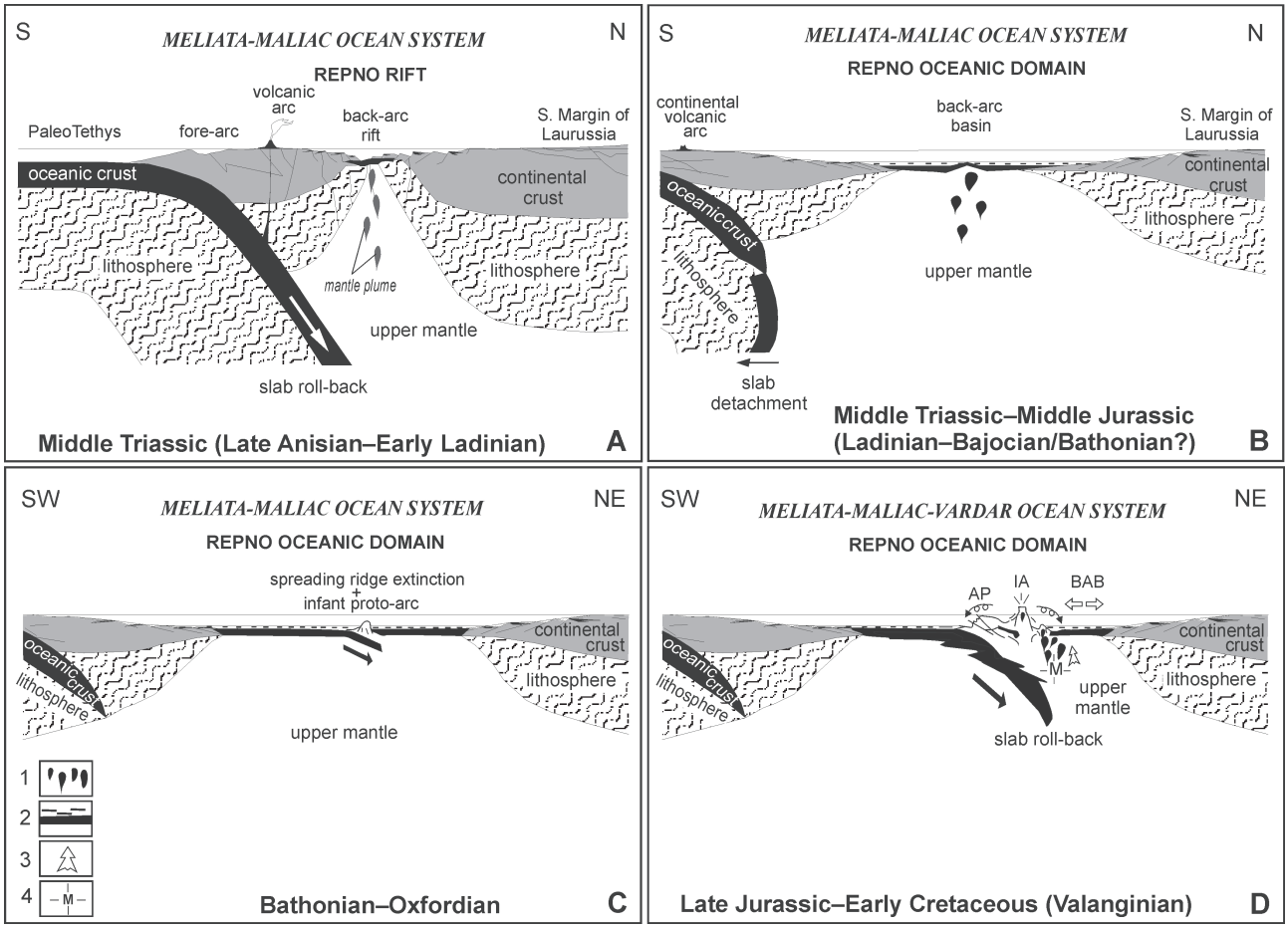

Fig. 12. Schematic geodynamic model for interaction of back-arc rifting, active spreading and subduction-related processes at the infant intra-oceanic arc setting for Mt Samoborska Gora and Medvednica Mt ophiolites in Repno oceanic domain as part of Meliata-Maliac-Vardar ocean system. **A** — the intracontinental back-arc rifting stage, **B** — the spreading stage and formation ensialic back-arc basin, **C** — the subduction stage of an active ocean ridge, **D** — the closure stage of the ROD. **1** — mantle diapires, **2** — oceanic crust with radiolarian cherts, **3** — raising of the mantle diapir, **4** — melting zone; **IA** = island arc (infant proto-arc/island arc system), **BAB** = back-arc basin, **AP** = accretionary prism.

the Albanide-Hellenide ophiolite mélanges, commenced by E-MORB (Saccani & Photiades 2005). The absence of E-MORB extrusives in the Mts Samoborska Gora and Medvednica ophiolite mélanges may indicate initially fast-spreading ridge segment of the ROD wherein interaction between the uprising asthenosphere and OIB-type enriched mantle source was suppressed to produce E-MORBs. Continuation of sea floor spreading during the Jurassic (Pliensbachian and Bajocian) produced N-MORB-like crust (Pamić 1997) in the ROD as a consequence of partial melting of pure suboceanic mantle with SSZ signatures inherited from an earlier (Hercynian?) subduction. The maximum evolved stage of spreading in the ROD is reflected by the Bathonian typical N-MORB extrusives (Slovenec & Lugović 2009).

(3) Intraoceanic convergence in the ROD commenced in the Late Bathonian–Early Callovian (Slovenec & Lugović 2009) as indicated also in the Mt Samoborska Gora ophiolite mélange, and may have continued until the Middle Callovian in the Mt Medvednica (Babić et al. 2002). Initial convergence led to formation of an extensional proto-arc basin in the leading edge of the oceanic lithophere overriding the still active oceanic ridge (Fig. 12C). This stage of partial melting generated N-MORB-like magmatism, similar to the spreading-ridge stage, and almost simultaneous medium-Ti magmatism in both Mts Samoborska Gora and Medvednica. Subsequent IAT magmas that reflect transition from incipient to true SSZ magmatism in the fore-arc basin are located only in the Mt Medvednica (Slovenec & Lugović 2009). It is most likely that the Mt Samoborska Gora ophiolite mélange represents a discrete segment of the ROD which records the shortest subduction related evolution. The oceanic crust fragments in the Kalnik Unit do not provide any evidence of formation of island arc in the ROD.

(4) The age and processes that led to the closure of the ROD are unclear and may be inferred only from the relevant metamorphic rocks assumed to represent the ancient ROD crust. The lower geenschist facies metamorphic complex of the Mt Medvednica formed by obduction of an island arc succession onto the Adria continental margin (Lugović et al. 2006) dated to 124–114 Ma ago (Belak et al. 1995) and a metamorphic sole from the Mt Kalnik which has a BABB-type crust protoliths (Ignjatić 2007), dated to 126–110 Ma,

suggest that the final closure most likely took place in Barremian–Aptian (Fig. 12D).

Conclusions

Our findings provide evidence that the Mt Samoborska Gora ophiolite mélange is the headmost edge of the Kalnik Unit which is obducted onto the Adria passive margin. It represents a discrete sector of the ROD which records a complexity of tectonomagmatic and sedimentary processes from the terminal intracontinental rifting in the Middle–Triassic (Illyrian–Fassanian) through various stages of back-arc spreading until the intraoceanic convergence in the Middle Jurassic (uppermost Bathonian–Early Callovian). From the incorporated clasts the stage(s) of spreading cannot be inferred properly in details. Intraocenic convergence led to formation of the crust in the upper plate by magmatism in an extensional proto-arc–fore-arc basin that was spreading over an active subducting ridge. This oceanic sector records the shortest duration of the convergence related evolution in the ROD which may have been suppressed before the true subduction commenced. The incorporated fragments were introduced into the mélange mostly by tectonically induced sedimentary processes in the accretionary wedge in the front of the proto-arc–fore-arc region, whilst older rocks, recognized by alkali basalts and Triassic limestones, repeatedly referred to as "exotic" in ophiolite mélanges, actually represent tectonic inclusions integrated in the trailing edge of the mélange in the latest phase of obduction.

Acknowledgments: This work is a contribution to the scientific projects Mesozoic magmatic, mantle and pyroclastic rocks of northwestern Croatia (Grant No. 181-1951126-1141 to Da.S.), Geological map of Republic of Croatia 1:50,000 (Grant No. 181-1811096-1093) and Tectonomagmatic correlation of fragmented oceanic lithosphere in the Dinarides (Grant No. 195-1951126-3205 to B.L.) carried out under the support of the Croatian Ministry of Science, Education and Sport. We are greatful to Špela Goričan for radioalarian analysis and Kadosa Balogh for K-Ar age determinations. We are also greatful to Tonći Grgasović and Radovan Filjak for assistance with rock sampling. Our thanks go to H.-P. Meyer and Rainer Altherr for microprobe facilities and Ilona Fin for excellent polished thin sections. Critical comments by Vesnica Garašić and Bruno Tomljenović improve an early version of the manuscript. Constructive reviews by Ján Spišiak and Dragan Milovanović greatly helped to achieve the final version of this paper.

References

Agrawal S., Guevara M. & Verma S.P. 2008: Tectonic discrimination of basic and ultrabasic volcanic rocks through log-transformed ratios of immobile trace elements. *Int. Geol. Rev.* 50, 1057–1079.

Babić Lj., Hochuli P.A. & Zupanič J. 2002: The Jurassic ophiolitic mélange in the NE Dinarides: Dating, internal structure and geotectonic implications. *Eclogae Geol. Helv.* 95, 263–257.

Bailey S.W. 1988: Chlorites: Structures and crystal chemistry. In: Bailey S.W. (Ed.): Hydrous phyllosilicates. *Rev. Miner., Miner. Soc. Amer.* 19, 347–403.

Balla Z. & Dobretsov N.L. 1984: Mineralogy and petrology of peculiar type Ophiolites — magmatic rocks from Szarvaskő (Bükk Mountains, North Hungary). *Ofioliti* 9, 107–122.

Bazylev B.A., Popević A., Karamata S., Kononkova N.N., Simakin S.G., Olujić J., Vujnović L. & Memović E. 2008: Mantle peridotites from the Dinaridic ophiolite belt and the Vardar zone western belt, central Balkan: A petrological comparison. *Lithos* 108, 37–71.

Beccaluva L., Piccardo G.B. & Serri G. 1980: Petrology of Northern Apennine ophiolites and comparision with other Tethyan ophiolites. In: Panayiotou A. (Ed.): Proceedings of the International Ophiolite Conference, Nicosia. *Geological Survey of Cyprus*, 314–331.

Beccaluva L., D.I. Girolamo P., Macciotta G. & Morra V. 1983: Magma affinities and fractionation trends in opholites. *Ofioliti* 8, 307–324.

Beccaluva L., Macciotta G., Piccardo G.B. & Zeda O. 1989: Clinopyroxene composition of ophiolite basalts as petrogenetic indicator. *Chem. Geol.* 77, 165–182.

Belak M., Pamić J., Kolar-Jurkovšek T., Pécskay Z. & Karan D. 1995: Alpine low-grade regional metamorphic complex of Mt. Medvednica (northwest Croatia). In: Vlahović I., Velić I. & Šparica M. (Eds.): Proceedings of the First Croatian Geological Congress, Opatija. *Inst. Geol.*, Zagreb, 67–70 (in Croatian, English summary).

Bébien J., Dimo-Lahitte A., Vergély P., Insergueix-Filippi D. & Dupeyrat L. 2000: Albanian ophiolites. I. Magmatic and metamorphic processes associated with the initiation of a subduction. *Ofioliti* 25, 39–45.

Bortolotti V. & Principi G. 2005: Tethyan ophiolites and Pangea break-up. *Island Arc* 14, 442–470.

Bortolotti V., Marroni M., Pandolfi L., Principi G. & Saccani E. 2002: Interaction between mid-ocean ridge and subduction magmatism in Albanian ophiolites. *J. Geol.* 110, 561–576.

Brajdić V. & Bukovec D. 1989: Spilitic rocks from Samobor mountains. *Geol. Vjes.* 42, 65–77 (in Croatian, English summary).

Cabanis B. & Lecolle M. 1989: Le diagramme La/10-Y/15-Nb/8: un outil pour la discrimination des series volcaniques et la mise en evidence des processus de mélange et/ou de contamination crustale. *C.R. Acad. Sci. Serr. II*, 309, 2023–2029.

Chen C.Y., Frey F.A. & Garcia M.O. 1990: Evolution of alkalic lavas at Haleakala Volcano, east Maui, Hawaii. *Contr. Mineral. Petrology* 105, 197–218.

Cousens B.L., Allan J.F. & Gorton M.P. 1994: Subduction-modified pelagic sediments as the enriched component in back-arc basalts from the Japan Sea: Ocean Drilling Program Sites 797 and 794. *Contr. Mineral. Petrology* 117, 421–434.

Crawford A. & Keays R.R. 1987: Petrogenesis of Victorian Cambrian tholeiites and implications for the origin of associated boninites. *J. Petrology* 28, 1075–1109.

Dilek Y., Furnes H. & Shallo M. 2007: Suprasubduction zone ophiolite formation along the periphery of Mesozoic Gondwana. *Gondvana Res.* 11, 453–475.

Ewart A., Bryan W.B., Chappell B.W. & Rudnick R.L. 1994: Regional geochemistry of the Lau-Tonga arc and back-arc systems. In: Hawkins J., Parson L. & Allan J. (Eds.): Proceedings of the Ocean Drilling Program. *Sci. Results* 135, 385–425.

Ewart A., Collerson K.D., Regelous M., Wendt J.I. & Niu Y. 1998: Geochemical evolution within the Tonga-Kermadec-Lau Arc-Back-arc System: the role of varying mantle wedge composition in space and time. *J. Petrology* 39, 331–368.

Fitton J.G. 2007: The OIB paradox. In: Foulger G.R. & Jurdy D.M. (Eds.): Plates, plume and planetary processes. *Geol. Soc. Amer., Spec. Pap.* 430, 387–412.

Fitton J.G., Kempton D., Ormerod D.S. & Leeman W.P. 1988: The

role of lithospheric mantle in the generation of late Cenozoic basic magmas in the western United States. *J. Petrology, Spec. Lithosphere Issue,* 331–349.

Goričan Š., Halamić J., Grgasović T. & Kolar-Jurkovšek T. 2005: Stratigraphic evolution of Triassic arc-backarc system in northwestern Croatia. *Bull. Soc. Géol. France* 176, 3–22.

Gribble R.F., Stern R.J., Newman S., Bloomer S.H. & O'Hearn T. 1998: Chemical and isotopic composition of Lavas from the Northern Mariana Trough: Implications for magmagenesis in back-arc basins. *J. Petrology* 39, 125–154.

Haas J. & Kovács S. 2001: The Dinaridic-Alpine connection — as seen from Hungary. *Acta Geol. Hung.* 44, 345–362.

Haas J., Mioč P., Pamić J., Tomljenović B., Árkai P., Bérczi-Makk A., Koroknai B., Kovács S. & R.-Felgenhauer E. 2000: Complex structural pattern of the Alpine-Dinaridic Pannonian triple junction. *Int. J. Earth Sci*. 89, 377–389.

Halamić J. 1998: Lithostratigraphy of Jurassic and Cretaceous sediments with ophiolites from the Mts. Medvednica, Kalnik and Ivanščica. *PhD. Thesis, Univ. Zagreb*, Zagreb, 1–188 (in Croatian, English summary).

Halamić J. & Goričan Š. 1995: Triassic radiolarites from Mts. Kalnik and Medvednica (Northwestern Croatia). *Geol. Croatica* 48, 129–146.

Halamić J., Slovenec Da. & Kolar-Jurkovšek T. 1998: Triassic pelagic limestones in pillow lavas in the Orešje quarry near Gornja Bistra, Medvednica Mt. (Northwest Croatia). *Geol. Croatica* 51, 33–45.

Hart S.R. & Brooks C. 1977: The geochemistry and evolution of Early Precambrian mantle. *Contr. Mineral. Petrology* 61, 109–128.

Hart W.K., Wolde G.C., Walter R.C. & Mertzman S.A. 1989: Basaltic volcanism in Ethiopia: constraints on continental rifting and mantle interactions. *J. Geophys. Res.* 94, 7731–7748.

Herak M. 1956: Geology of the Mts. Samoborska Gora. *Acta Geol.* 1, 49–73 (in Croatian, German summary).

Hoeck V., Koller F., Meisel T., Onuzi K. & Kneringer E. 2002: The Jurassic South Albanian ophiolites: MORB- vs. SSZ-type ophiolites. *Lithos* 65, 143–164.

Ignjatić S. 2007: Upper Cretaceous amphibolites from lherzolite metamorphic sole (Kalnik Mt., Croatia). *Graduation Thesis, Univ. Zagreb*, Zagreb, 1–61 (in Croatian, English summary).

Ikeda Y. & Yuasa M. 1989: Volcanism in nascent back-arc basin behind the Shichito Ridge and adjacent areas in the Izu-Ogaswara arc, northwest Pacific. *Contr. Mineral. Petrology* 101, 377–393.

Jahn B. 1986: Mid-ocean ridge or marginal basin origin of the East Taiwan Ophiolite: chemical and isotopic evidence. *Contr. Mineral. Petrology* 92, 194–206.

Kent R., Storey M. & Saunders A.D. 1992: Large igneous provinces: sites of plume impact or plume incubation. *Geology* 20, 891–894.

Kloc I. 2005: The ophiolitic rocks of Samoborska Gora. *Graduation Thesis, Univ. Zagreb*, Zagreb, 1–65 (in Croatian, English summary).

Komiya T., Maruyama S., Hirata T., Yurimoto H. & Nohda S. 2004: Geochemistry of the oldest MORB and OIB in the Isua Supracrustal Belt, southern west Greenland: Implications for the composition and temperature of early Archean upper mantle. *Island Arc* 13, 47–72.

Kostopoulos D.K. & James S.D. 1992: Parameterization of the melting regime of the shallow upper mantle and the effects of variable lithospheric stretching on mantle modal stratification and trace element concentrations in magmas. *J. Petrology* 33, 665–691.

Leat P.T., Livermore R.A., Millar I.L. & Pearce J.A. 2000: Magma supply in back-arc spreding centre segment E2, East Scotia Ridge. *J. Petrology* 41, 845–866.

Leterrier J., Maury R.C., Thonon P., Girrard D. & Marchal M. 1982: Clinopyroxene composition as a method of identification of the magmatic affinities of paleovolcanic series. *Earth Planet. Sci Lett*. 59, 139–154.

Liou J.G., Maruyama S. & Cho M. 1987: Very low-grade metamorphism of volcaniclastic rocks-mineral assemblages and mineral-facies. In: Frey M. (Ed.): Very low-grade metamorphism. *Blackie and Son*, New York, 59–113.

Lugović B., Altherr R., Raczek I., Hofmann A.W. & Majer V. 1991: Geochemistry of peridotites and mafic igneous rocks from the Central Dinaric Ophiolite Belt, Yugoslavia. *Contr. Mineral. Petrology* 106, 201–216.

Lugović B., Šegvić B. & Altherr R. 2006: Petrology and tectonic significance of greenschists from the Medvednica Mts. (Sava unit, NW Croatia). *Ofioliti* 31, 39–50.

Lugović B., Slovenec Da., Halamić J. & Altherr R. 2007: Petrology, geochemistry and geotectonic affinity of the Mesozoic ultramafic rocks from the southwesternmost Mid-Transdanubian Zone in Croatia. *Geol. Carpathica* 58, 511–530.

McKenzie D. & Bickle M.J. 1988: The volume and composition of melt generated by extension in the lithosphere. *J. Petrology* 29, 625–679.

Monjoie P., Lapierre H., Tashko A., Mascle G.H., Dechamp A., Muceku B. & Brunet B. 2008: Nature and origin of the Triassic volcanism in Albania and Othrys: a key to understanding the Neotethys opening? *Bull. Soc. Géol. France* 179, 411–425.

Morgan W.J. 1981: Hotspot tracks and the opening of the Atlantic and Indian Oceans. In: Emiliani C. (Ed.): The oceanic lithosphere. *Wiley*, New York, 443–487.

Morimoto N. 1988: Nomenclature of pyroxenes. *Schweiz. Mineral. Petrolog. Mitt*. 68, 95–111.

Münker C. 2000: The isotope and trace element budget of the Cambrian Devil River arc system, New Zealand: Identification of four source components. *J. Petrology* 41, 759–788.

Nisbet E.G. & Pearce J.A. 1977: Clinopyroxene composition in mafic lavas from different tectonic settings. *Contr. Mineral. Petrology* 63, 149–160.

Okamura S., Arculus R.J. & Martynov Y.A. 2005: Cenozoic magmatism of the North-Eastern Eurasian Margin: The role of lithosphere versus astenosphere. *J. Petrology* 46, 221–253.

Palinkaš L.A., Bermanec V., Moro A., Dogančić D. & Strmić-Palinkaš S. 2006: The northernmost Ni-lateritic weathering crust in the Tethyan domain, Gornje Orešje, Medvednica Mt. *Proceed., Mesozoic ophiolite belts of northern part of the Balkan Peninsula*, Belgrade-Banja Luka, 97–101.

Pamić J. 1997: The northwesternmost outcrops of the Dinaridic ophiolites: a case study of the Mt. Kalnik (North Croatia). *Acta Geol. Hung.* 40, 37–56.

Pamić J. 2000: The Periadriatic-Sava-Vardar Suture Zone. In: Vlahović I. & Biondić R. (Eds.): Proceedings of the Second Croatian Geological Congress, Cavtat-Dubrovnik. *Inst. Geol*., Zagreb, 333–337.

Pamić J. 2002: The Sava-Vardar Zone of the Dinarides and Hellenides versus the Vardar ocean. *Eclogae Geol. Helv*. 95, 99–113.

Pamić J. & Tomljenović B. 1998: Basic geological data on the Croatian part of the Mid-Transdanubian Zone as exemplified by Mt. Medvednica located along the Zagreb-Zemplín Fault Zone. *Acta Geol. Hung.* 41, 389–400.

Pearce J.A. 1983: Role of the sub-continental lithosphere in magma genesis at active continental margins. In: Hawkesworth C.J. & Norry M.J. (Eds.): Continental basalts and mantle xenoliths. *Shiva*, Nantwich, 230–249.

Pearce J.A. 2003: Supra-subduction zone ophiolites: The search for modern analogues. In: Dilek Y. & Newcomb S. (Eds.): Ophiolite concept and the evolution of geological thought. *Geol. Soc. Amer. Spec. Pap., Geol. Soc. Amer., Boulder, CO*, 373, 269–293.

Pearce J.A. & Cann J.R. 1973: Tectonic setting of basic volcanic rocks determined using trace element analysis. *Earth Planet. Sci. Lett*. 19, 290–300.

Pearce J.A. & Norry M.J. 1979: Petrogenetic implications of Ti, Zr, Y, and Nb variations in volcanic rocks. *Contr. Mineral. Petrology* 69, 33–47.

Pearce J.A. & Wanming D. 1988: The ophiolites of the Tibetan Geotraverses, Lhasa to Golmud (1985) and Lhasa to Kathmandu (1986). *Phil. Trans. Roy. Soc. London* 327, 215–238.

Pearce J.A., Baker P.E., Harvey P.K. & Luff I.W. 1995: Geochemical evidence for subduction flukses, mantle melting for fractional crystallization beneath the South Sandwich Island Arc. *J. Petrology* 36, 1073–1109.

Peate D.W., Pearce J.A., Hawkesworth C.J., Colley H., Edwards M.H. & Hirose K. 1997: Geochemical variations in Vanuatu Arc Lavas: the role of subducted material and a variable mantle wedge composition. *J. Petrology* 38, 1331–1358.

Perry F.V., Baldridge W.S., DePaolo D.J. & Shafiqullah M. 1990: Evolution of a magmatic system during continental extension: the Mount Taylor volcanic field, New Mexico. *J. Geophys. Res.* 95, 19327–19348.

Placer L. 1999: Contribution of the macrotectonic subdivision of the border region between Southern and External Dinarides. *Geologija* 41, 223–255.

Pouchou J.L. & Pichoir F. 1984: A new model for quantitative analyses. I. Application to the analysis of homogeneous samples. *La Recherche Aérospatiale* 3, 13–38.

Pouchou J.L. & Pichoir F. 1985: "PAP" (φ-ρ-Z) correction procedure for improved quantitative microanalysis. In: Armstrong J.T. (Ed.): Microbeam analysis. *San Francisco Press*, 104–106.

Robertson A., Karamata S. & Šarić K. 2009: Overwiew of ophiolites and related units in the Late Palaeozoic–Early Cenozoic magmatic and tectonic development of Tethys in the northern part of the Balkan region. *Lithos* 108, 1–36.

Saccani E. & Photiades A. 2005: Petrogenesis and tectonomagmatic significance of volcanic and subvolcanic rocks in the Albanide-Hellenide ophiolitic mélanges. *The Island Arc* 14, 494–516.

Saunders A.D. & Tarney J. 1979: The geochemistry of basalts from a back-arc spreading center in the East Scotia Sea. *Geochim. Cosmochim. Acta* 43, 555–572.

Sayit K. & Göncüoğlu M.C. 2009: Geochemistry of mafic rocks of the Karakaya complex, Turkey: evidence for plume-involvement in the Palaeotethyan extensional regime during the Middle and Late Triassic. *Int. J. Earth Sci*. 98, 367–385.

Schmid S.M., Bernoulli D., Fügenschuh B., Matenco L., Scheffer S., Schuster R., Tischler M. & Ustaszewski K. 2008: The Alpine-Carpathian-Dinaridic orogenic system: correlation and evolution of tectonic units. *Swiss J. Geosci*. 101, 139–183.

Serri S. 1981: The petrochemistry of ophiolitic gabbro-complexes: A key for classification of ophiolites to low-Ti and high-Ti types. *Earth Planet. Sci. Lett*. 52, 203–212.

Shervais J.W. 1982: Ti-V plots and petrogenesis of modern and ophiolitic lavas. *Earth Planet. Sci. Lett*. 59, 101–118.

Shervais J.W. 2001: Birth, dead, and resurrection: The life cycle of supra-subduction zone ophiolites. *Geochem., Geophys., Geosci.* 2 [2000GC000080].

Slovenec Da. & Lugović B. 2008: Amphibole gabbroic rocks from the Mt Medvednica ophiolite mélange (NW Croatia): geochemistry and tectonic setting. *Geol. Carpathica* 59, 277–293.

Slovenec Da. & Lugović B. 2009: Geochemistry and tectono-magmatic affinity of extrusive and dyke rocks from the ophiolite mélange in the SW Zagorje-Mid-Transdanubian Zone (Mt. Medvednica, Croatia). *Ofioliti* 34, 63–80.

Slovenec Da. & Pamić J. 2002: The Vardar Zone ophiolites of Mt Medvednica located along the Zagreb-Zemplín line (NW Croatia). *Geol. Carpathica* 53, 53–59.

Spath A., Le Roex A.P. & Duncan R.A. 1996: The geochemistry of lavas from the Comores Archipelago, Western Indian Ocean: petrogenesis and mantle source region characteristics. *J. Petrology* 37, 961–991.

Spath A., Le Roex A.P. & Opivo-Akech N. 2001: Plume lithosphere interaction and the origin of continental rift-related alkaline volcanism the Chyulu Hills volcanic Province, Soutern Kenya. *J. Petrology* 42, 765–787.

Stampfli G.M. & Borel G.D. 2002: A plate tectonic model for the Paleozoic and Mesozoic constrained by dynamic plate boundaries and restored synthetic ocean isochrons. *Earth Planet. Sci. Lett*. 196, 17–33.

Stampfli G.M. & Borel G.D. 2004: The TRANSMED transects in space and time: Constraints on the paleotectonic evolution of the Mediterranean domain. In: Cavazza W., Roure F., Spakman W., Stampfli G.M. & Ziegler P.A. (Eds.): The TRANSMED Atlas: the Mediterranean Region from crust to mantle. *Springer Verlag*, 53–80.

Stern C. 2004: Subduction initiation: Spontaneous and induced. *Earth Planet. Sci. Lett.* 226, 275–292.

Sun S.S. & McDonough W.F. 1989: Chemical and isotopic systematics of oceanic basalts: implications for mantle composition and processes. In: Saunders A.D. & Norry M.J. (Eds.): Magmatism in ocean basins. *Geol. Soc. London., Spec. Publ*. 42, 313–345.

Šikić K. & Basch O. 1975: Geological events from Paleozoic to Quaternary in the western part of Zagreb area. *2rd god. znanstveni skup sekcije za primjenu geol., geofiz., geokem. Znanstv. savjeta za naftu JAZU (A), Zagreb*, 5, 69–86 (in Croatian, English summary).

Šikić K., Basch O. & Šimunić An. 1978: Basic geological map 1:100,000. Sheet Zagreb. *Inst. Geol. Istraž. Zagreb, Sav. Geol. Zavod*, Beograd.

Šikić K., Basch O. & Šimunić An. 1979: Basic geological map 1:100,000. Sheet Zagreb, explanatory notes. *Inst. Geol. Istraž. Zagreb, Sav. Geol. Zavod*, Beograd, 1–81 (in Croatian, English summary).

Tari V. & Pamić J. 1998: Geodynamic evolution of the Northern Dinarides and the southern parts of the Pannonian Basin. *Tectonophysics* 297, 296–281.

Taylor S.R. & McLennan S.M. 1985: The continental crust: its composition and evolution. *Blackwell*, Oxford, 1–312.

Thomson Jr. J.B. 1991: Modal space: Applications to ultramafic and mafic rocks. *Canad. Mineralogist* 29, 615–632.

Tomljenović B. 2002: Structural characteristics of Medvednica and Samoborsko Gorje Mts. *PhD. Thesis, Univ. Zagreb*, Zagreb, 1–206 (in Croatian, English summary).

Tomljenović B., Csontos L., Márton E. & Márton P. 2008: Tectonic evolution of the northwestern Internal Dinarides as constrained by structures and rotation of Medvednica Mountains, North Croatia. *Geol. Soc. London, Spec. Publ.* 298, 145–167.

Tracy R.J. & Robinson P. 1977: Zoned titanium augite in alkali olivine basalt from Tahiti and the nature of titanium substitutions in augite. *Amer. Mineralogist* 62, 634–645.

Weaver D.S., Saunders A.D., Pankhurst R.J. & Tarney J. 1979: A geochemical tudy of magmatism associated with the initial stages of back-arc spreading. *Contr. Mineral. Petrology* 68, 151–169.

Wilson M. 1989: Igneous petrogenesis. *Unwin Hyman Ltd*., London, 1–465.

Winchester J.A. & Floyd P.A. 1977: Geochemical discrimination of different magma series and their differentiation products using immobile elements. *Chem. Geol.* 20, 325–343.

Wood D.A. 1980: The application of a Th-Hf-Ta diagram to problems of tectonomagmatic classification and establishing the nature of crustal contamination of basaltic lavas of the British Tertiary volcanic province. *Earth Planet. Sci. Lett*. 50, 11–30.

Zindler A. & Hart S.R. 1986: Chemical geodynamics. *Ann. Rev. Earth Planet. Sci.* 14, 439–571.